Università degli Studi di Padova

Dipartimento di Biologia

Corso di Laurea Magistrale in Biotecnologie Industriali

Design of experiment to increase lipid and pigment production in *Chromochloris zofingiensis*: lab and pilot scale cultivation

Relatore: Prof.ssa Eleonora Sforza

Dipartimento di Ingegneria industriale

Correlatore: Dr. Ing. Felix Krujatz

Bioprocess Engineering Department

Controrelatore: Prof.ssa Michela Zottini

Dipartimento di Biologia

Laureando: Agnese Torrisi

Anno Accademico 2022/2023

It’s not love or money that makes the world go round, it’s photosynthesis (Richmond, 2007).

Abstract

Microalgae are proving to be one of the most promising sustainable food sources of the future, characterised by high nutritional value with proven health benefits. Within this context, the chlorophyte *Chromochloris zofingiensis* is increasingly gaining the attention of the scientific community, because of its rapid growth, trophic flexibility and simultaneous synthesis of high amounts of triglycerides and carotenoids in response to various stress-inducing conditions (e.g. nitrogen limitation/starvation, salt stress). Furthermore, the additional production of the powerful antioxidant astaxanthin makes *C. zofingiensis* a potential alternative producer to the microalga *Haematococcus pluvialis*. The initial cultivation of *Chromochloris zofingiensis* in a 200-L pilot-scale PBR revealed significant contributions of nitrogen limitation and salinity stress on the accumulation of carotenoids and consistently astaxanthin, with a dynamic not fully clear. Subsequent experiments conducted in smaller scale flat-plate PBRs operated in continuous mode revealed that, when a one-step approached is applied, the addition of sodium chloride, unlike nitrogen limitation, resulted in an increase in carotenoid content and relative productivity, without significantly affecting biomass growth. Based on the different results obtained under the two culture conditions, a more rational approach is needed to ascertain the combined effect of different stresses on biomass growth and carotenoid and lipid production. For these reasons, a design of experiment (DoE) statistical approach to the CellDEG© high-density cultivation system was applied. Here, DoE results regarding biomass, showed that light intensity, followed by nitrogen limitation and salt stress, was the main variable influencing the biomass growth.

Table of contents

Chapter 1: Introduction

1.1 Microalgae as alternative food source of the future

The global population is rapidly expanding, projected to reach 9.5 billion by 2050, raising critical concerns regarding food security and malnutrition. To meet the rising global demand for food, the agricultural sector requires considerable transformation. This includes expanding agricultural areas, implementing crop rotations, and adopting advanced technologies to boost yields. However, these measures come with high costs and contribute to existing issues such as soil degradation, deforestation, eutrophication, and biodiversity loss. Considering these challenges, there is a need for an alternative source that is easily producible, cost-effective, and capable of intensive production at large scale of valuable bioactive metabolites and nutrients (Kusmayadi *et al*. 2021a; Kaur *et al*. 2023).

In this context, microalgae are emerging as a viable and sustainable food solution. Compared to other microorganisms and terrestrial plants, they possess several unique advantages that have captured the interest of researchers across diverse fields such as environmental sciences, biology, genetics, chemistry, chemical engineering, medicine, polymer science, agriculture, and aquaculture (Daneshvar *et al*. 2021a; Kaur *et al*. 2023). Microalgae exhibit significantly higher photosynthetic efficiency compared to terrestrial plants, leading to increased growth rates and productivity per hectare (Lari and Khosravitabar 2020). Unlike plants, microalgae are not restricted to arable lands and freshwater sources. They can be cultivated on unproductive lands, including infertile, arid, semi-arid areas, and polluted soils unsuitable for traditional agriculture. Additionally, these microorganisms can thrive in saline water and nutrient-enriched wastewater. Furthermore, microalgae cultivation is not limited by seasons; it can be carried out year-round and harvested daily in certain geographical area or indoor (Christaki, Florou-Paneri, and Bonos 2011; Lari and Khosravitabar 2020; Daneshvar *et al*.

2021b). Besides these considerations, it is mainly due to their rich biochemical composition, characterised by high-quality functional components, that microalgae are emerging as the sustainable food source of the future (Kusmayadi *et al*. 2021b).

1.2 Microalgae

Microalgae are eukaryotic unicellular photosynthetic organisms that possess, like higher plants, the ability to convert light energy into chemical energy, contributing to the production of approximately 50% of Earth's assimilable oxygen (Khan, Shin, and Kim 2018; Alejandro Reza-Solis *et al*. 2023). These microorganisms exhibit diverse shapes and sizes, ranging from a few to several hundred micrometres, depending on their class and species (Kratzer and Murkovic 2021). Microalgae are further subdivided into various classes, including *Chlorophyceae* (green algae), *Chrysophyceae* (golden algae), *Rhodophyceae* (red algae), *Phaeophyceae* (brown algae), and *Bacillariophyceae* (diatoms) (Zuccaro *et al*. 2020). They are ubiquitously distributed across various ecosystems, thanks to their remarkable capacity to thrive in a wide range of conditions characterised by varying levels of salinity, temperature, substrates and pH (Khan, Shin, and Kim 2018; Alejandro Reza-Solis *et al*. 2023). They have gained significant global attention owing to their versatile applications in the renewable energy, biopharmaceutical, and nutraceutical sectors. Microalgae offer a renewable and sustainable resource, contributing to the production of an extensive range of bioproducts, including polysaccharides, lipids, pigments, proteins, vitamins, bioactive compounds, and antioxidants (Andersen and Phycological Society of America 2009; Khan, Shin, and Kim 2018).

Microalgae cultivation can be achieved through a variety of metabolic pathways, including photoautotrophic, heterotrophic, and mixotrophic approaches, and can be facilitated by different cultivation systems, primarily categorised as open and closed systems (Ahmad *et al*. 2021). Key parameters critical for the regulation of

microalgal growth encompass light, temperature, pH, nutrient availability, gas exchange, and salinity. Additionally, factors like stirring and mixing, the dimensions of the bioreactor in terms of width and depth, harvest frequency, and dilution rate are also crucial determinants of the overall success of microalgal cultures (Khan, Shin, and Kim 2018; Vale *et al*. 2020).

1.2.1 Nutrients

Microalgal cultures necessitate a supply of macronutrients and trace elements in sufficient quantities and in chemically accessible forms. Among these, nitrogen, phosphorus, and carbon serve as the foundational elements for microalgal growth and are categorised as crucial macronutrients (Khan, Shin, and Kim 2018).

Carbon is the predominant element in microalgal biomass, constituting up to 65% of its dry weight (Zuccaro *et al*. 2020). It is absolutely vital for photosynthesis, thereby influencing algal growth and reproduction significantly. Microalgae can utilise carbon in various forms: CO_2, carbonate, or bicarbonate for autotrophic growth, and acetate or glucose for heterotrophic growth. The availability of inorganic carbon in water can take on different forms depending on factors like pH, temperature, and nutrient content:

$$CO_2 + H_2 \leftrightarrow H_2CO_3 \leftrightarrow H^+ + HCO_3^- \leftrightarrow 2H^+ + CO_3^{2-}$$

As pH increases, carbonate concentrations rise while molecular CO_2 and bicarbonate concentrations decrease (Juneja, Ceballos, and Murthy 2013; Mohsenpour *et al*. 2021).

Nitrogen, constituting approximately 7–10% of the cell's dry weight, stands as the second most prevalent element in microalgal biomass. It plays an essential role in a wide range of cellular components, including proteins, amino acids, amides, DNA, RNA, alkaloids, and enzymes (Ravindran *et al*. 2016). Microalgae possess the capability to utilise nitrogen from a diverse range of sources, including inorganic sources such as NH_4^+, NO_3, and NO_2, as well as organic sources like amino acids, urea, purines, and nucleosides (Richmond 2007; Mohsenpour *et al*. 2021).

Phosphorus is another crucial element in microalgae, participating in numerous metabolic pathways and serving as a structural component within phospholipids, nucleotides, and ATP (Mohsenpour *et al*. 2021). Despite the fact that phosphorus makes up less than 1% of algal biomass, it frequently stands as one of the most critical growth-limiting factors in algal biotechnology. This is primarily due to its propensity to readily bind with other ions, such as CO_3^{2-} and iron, leading to its precipitation and, consequently, rendering this essential nutrient inaccessible for algal uptake. The preferred form of phosphorus supplied to algae is typically in the form of orthophosphate (PO_4^{2-}) (Richmond 2007).

Microalgal growth also requires macronutrients like Na, Mg, Ca, and K; Additionally, micronutrients such as Mo, Mn, B, Co, Fe, and Zn, along with various trace elements, are essential for their growth and metabolic processes (Khan, Shin, and Kim 2018).

1.2.2 Light

In photosynthetic cultures of microalgae, three critical attributes of light - intensity, wavelength, and photoperiod (day-night cycle) - play pivotal roles in shaping the growth, biochemical composition, and biomass yield of these microorganisms (Khan, Shin, and Kim 2018; Daneshvar *et al*. 2021b).

There is a fundamental relationship between light intensity (I) and rate of photosynthesis (P) and is illustrated by the photosynthetic light-response curve. This curve consists of three distinct phases: light-limitation, light-saturation, and photoinhibition phase (Fig. 1.1)

At low light intensities ($I < I_k$), the rate of photosynthesis typically exhibits a linear relationship with light intensity because photosynthesis is limited by the rate at which photons are captured. This condition of light limitation occurs in cultures characterised by inadequate light intensity.

When light intensity reaches a saturation threshold (I_k), microalgae become 'light-saturated' ($I_k < I < I_{inhib}$). In this state, the rate of photosynthesis is generally at its

maximum and no longer influenced by variations in light intensity. Instead, it becomes limited by the subsequent reactions following photon capture.

If light intensity continues to rise beyond an inhibitory threshold (I_{inhib}) ($I > I_{inhib}$), the rate of photosynthesis starts to decline with light intensity which, above a certain point can inflict damage on crucial proteins within the photosynthetic apparatus (Khan, Shin, and Kim 2018; Béchet, Shilton, and Guieysse 2013; Daneshvar *et al*. 2021b).

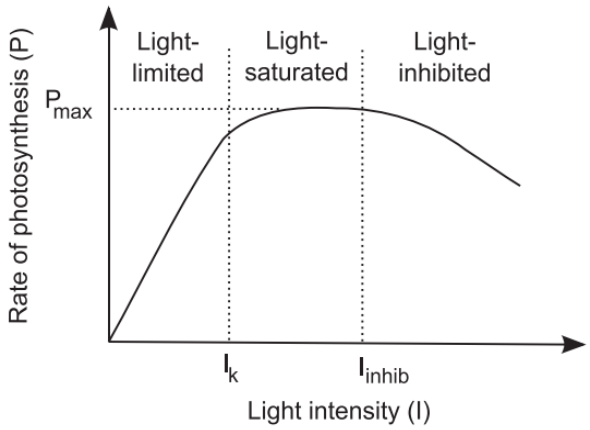

Fig. 1.1 Typical PI relationship showing the distinct phases of microalgae's response to light (Béchet *et al*., 2013)

Ensuring proper light penetration and uniform distribution is essential to prevent photoinhibition, also known as the self-shading effect, where lower layers of algae are shaded by upper layers. Photoinhibition can be mitigated by increasing light intensity or continuously mixing the culture. As a result, determining the ideal light intensity requires experimental evaluation in each case to maximise CO_2 assimilation while minimising photorespiration and photoinhibition. The optimal light intensities for the growth of most microalgae species typically range from about 200 to 400 µmol m^{-2} s^{-1} (Khan, Shin, and Kim 2018).

1.2.3 Temperature, pH and mixing

Temperature exerts a direct impact on various aspects of microalgae, including metabolism, nutrient absorption, CO_2 fixation, photosynthesis, and growth rate. Beyond growth, temperature also plays a pivotal role in shaping the physiology and biochemical composition of microalgae (Daneshvar *et al*. 2021b). Moreover, temperature can be strategically employed as a stress treatment to stimulate the production of valuable metabolites (Khan, Shin, and Kim 2018). Generally, most microalgae species can thrive within a temperature range spanning from 10°C to 30°C, although the optimal temperature typically falls within a narrower range, often between 15°C and 25°C (Mohsenpour *et al*. 2021).

The pH of the culture medium stands as another crucial factor influencing the metabolism and growth of microalgae. The pH level governs the acid-base equilibrium within the cultivation medium, impacting the solubility and accessibility of various forms of inorganic carbon (such as CO_2, bicarbonate, and carbonate) and nutrients (including phosphates and ammonium/ammonia), as well as their liquid–gas transfer phenomena (Daneshvar *et al*. 2021b). Different microalgae species have varying pH requirements. The majority thrive within a pH range that typically spans from 6 to 8.76 (Khan, Shin, and Kim 2018).

Furthermore, mixing and aeration play crucial roles in ensuring the even distribution of nutrients, air, and CO_2 within microalgae cultures, as well as the removal of O2 excess. They also facilitate the penetration and uniform dispersion of light throughout the culture, preventing biomass settling and the formation of aggregates (Khan, Shin, and Kim 2018; Ahmad *et al*. 2021).

1.3 Trophic modes

In terms of the energy and carbon sources employed for their metabolic processes, microalgae have the capacity to thrive through three distinct methods: autotrophic growth, heterotrophic growth, and mixotrophic growth (Fig. 1.2) (Daneshvar *et al*. 2021b).

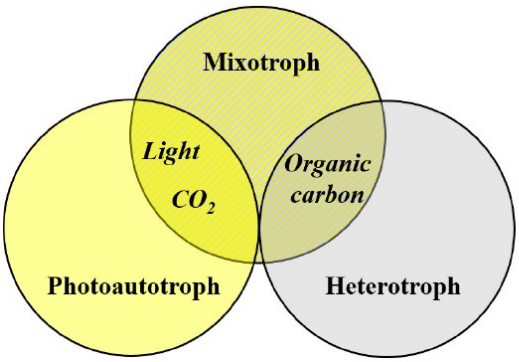

Fig. 1.2 Energy and carbon sources of microalgae (Kratzer *et al*., 2021)

1.3.1 Autotrophic Cultivation

Autotrophic cultivation stands as the predominant growth method for microalgae. Autotrophs possess the ability to convert both physical (photons) and chemical (CO_2 and H_2O) energy sources into organic matter. Specifically, photoautotrophic microalgae harness light to produce ATP and NADPH, which are subsequently used in the Calvin-Benson cycle to generate glucose. This glucose serves as a fundamental building block for various metabolic pathways to generate other compounds like proteins, complex carbohydrates and lipids. These autotrophic organisms are notably self-sufficient and self-sustaining, owing to their capacity to derive energy from sunlight (Lari and Khosravitabar 2020). Light can be provided in the form of sunlight or through artificial means, such as light-emitting diodes (LEDs) (Zuccaro *et al*. 2020).

One of the primary advantages of employing the photoautotrophic mode in microalgae cultivation is the capture of atmospheric CO_2 (Vale *et al*., 2020). A further advantage is the lower risk of contamination by bacteria and fungi compared to other trophic modes. Consequently, large-scale outdoor microalgae cultivation setups, such as open ponds, typically operate under photoautotrophic conditions (Daneshvar *et al*. 2021b). On the other side, the main drawback of photoautotrophic cultivation lies in its dependence on light. The need for a high

surface area to volume ratio (A/V) in photobioreactors poses an additional challenge in this mode. In autotrophic cultivation shading becomes another critical limiting factor for algal growth, especially when an adequate mixing system is lacking. Nevertheless, due to its readily available energy sources, the photoautotrophic cultivation strategy appears economically viable (Lari and Khosravitabar 2020).

1.3.2 Heterotrophic Cultivation

Heterotrophic organisms rely on organic carbon substrates as their primary sources of energy for growth and survival (Ahmad *et al*. 2021).

Heterotrophic cultivation of microalgae presents several advantages compared to other trophic modes, including light-independency, simplifying the design of photobioreactors, as they require a high surface A/V ratio in such conditions. Other pros include precise control over the cultivation process, increased growth rates, and enhanced lipid productivity, due to high availability of carbon source in the cultures. Boosting biomass and lipid productivity under heterotrophic conditions leads to reduced harvesting expenses. However, one of the primary drawbacks is the cost associated with supplementing the culture media with organic materials (glucose, acetate, and glycerol). Using carbon-rich wastewater as an alternative to pure organic materials in the cultivation media could be a viable solution to lower production costs. Nonetheless, this approach comes with potential challenges, such as the risk of microbial contamination due to the presence of organic substrates and water. Decontamination would be an additional step, incurring extra costs and labour in the microalgae culture process. It's also important to consider that dark conditions in heterotrophic cultivation may inhibit pigmentation and secondary metabolite production (Lari and Khosravitabar 2020; Ahmad *et al*. 2021; Daneshvar *et al*. 2021b).

1.3.3 Mixotrophic Cultivation

Microalgae also have the capability to operate in a mixotrophic mode, which combines elements of both autotrophy and heterotrophy (Daneshvar *et al*. 2021b). Mixotrophic growth involves the simultaneous assimilation of both CO_2 and organic carbon, enabling the concurrent operation of respiratory and photosynthetic metabolic processes (Lari and Khosravitabar 2020). Under mixotrophic conditions, the availability of light energy is not a limiting factor for cell growth and productivity, unlike in photoautotrophy. Additionally, microalgal cells could maintain light-dependent biosynthesis of some valuable products like pigments and carotenoids, different from heterotrophy. Unlike heterotrophy, mixotrophic cultivation of microalgae also contributes to the goal of CO_2 sequestration. In this model, during the initial phase, the presence of a high level of organic carbon in the medium induces heterotrophic conditions. As the organic carbon is depleted to a certain level, the autotrophic growth is induced and the assimilation of organic carbon is initiated (Khan, Shin, and Kim 2018; Lari and Khosravitabar 2020; Daneshvar *et al*. 2021b).

1.4 Cultivation strategies

Microalgae can be cultivated using a variety of techniques. The batch approach is the simplest, cheapest and most common in large scale systems. It involves no input or output of material, meaning that this system's resources are finite and that microalgal growth occurs until the exhaustion of some limiting factor. In continuous systems, on the contrary, fresh medium is constantly introduced into the culture at a rate corresponding to the removal of the culture broth, ensuring a constant growth rate. Additionally, a semi-continuous culture approach can be employed by combining elements of both methods (Fernandes *et al*. 2015; Lari and Khosravitabar 2020).

1.4.1 Batch cultures

More specifically, in a batch culture, an inoculum with a fixed volume of nutrient media is charged into the system. This type of approach exhibits five distinct growth phases (Fig. 1.3):

(1) Lag: During this initial phase, there is a physiological adjustment to the new environment. The duration of the lag phase depends on the size of the inoculum and the environmental conditions. It can be shortened if cells from a later exponential growth phase are used as the inoculum or if cells have already been adapted to the culture conditions.

(2) Exponential: In this phase, the cells start to grow and multiply exponentially over time, provided that mineral substrates and light energy are abundant.

(3) Declining relative growth: This phase occurs when a growth requirement for cell division is limiting.

(4) Stationary: During this phase, cell division slows down, and biomass accumulates at a constant rate due to a lack of resources needed for further growth.

(5) Death/lysis: In this final phase, cells begin to die due to a shortage of nutrients (Richmond 2007).

Batch cultures are typically harvested just before entering the stationary phase. However, the quality of the harvest can be less predictable compared to continuous systems and may vary depending on the timing of the harvest (Vale *et al*. 2020).

Although this method is simple and cost-effective, it comes with several drawbacks. It requires downtime for reactor cleaning and startup between cycles, leading to decreased productivity and greater demands for labour, water, and chemicals. In addition to this, high harvesting costs due to low cell concentrations, uncertain reliability and variable product quality must be considered. As a result, batch cultivation may not be the most suitable option for large-scale microalgae biomass production. Nonetheless, these challenges can be addressed through semi-continuous and continuous cultivation methods (Fernandes *et al*. 2015).

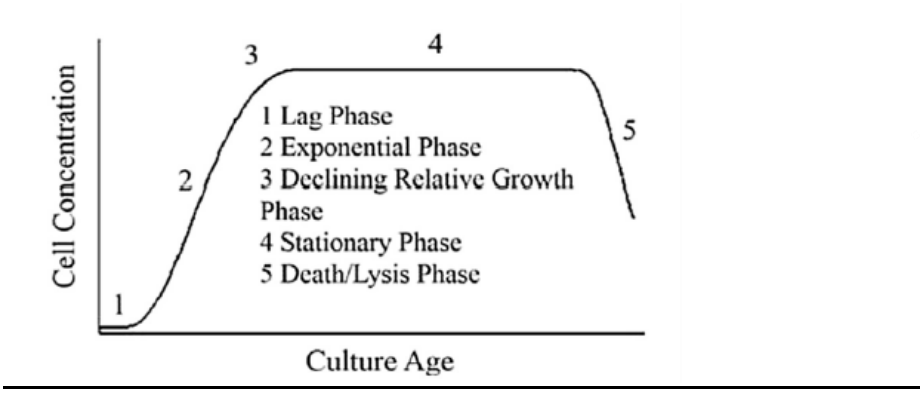

Fig. 1.3 Schematic growth curve of a microalgal batch culture system (Abu Yousuf, 2020)

1.4.2 Continuous cultures

In a continuous system (Fig. 1.4), the increase in biomass concentration in the culture can be expressed as the difference between biomass growth and biomass removal from the bioreactor over a given period of time (Richmond 2007). For an infinitesimally small time interval, the mass balance can be expressed as:

$$V * dC_X/dT = \mu C_X * V + F_{in} * C_{Xin} - F_{out} * C_{Xout} \quad \text{Eq.1}$$

Where V represents the working volume (L); dC_X/dt is the biomass accumulation inside the bioreactor (g L^{-1} h^{-1})); μ represents specific growth rate (h^{-1}); C_X is the biomass concentration (g L^{-1}); F_{in} and F_{out} the volumetric inflow and outflow rates (L h^{-1}) (Richmond 2007; Fernandes *et al*. 2015).

Under the following assumptions: (i) constant flow ($F = F_{in} = F_{out}$); (ii) constant volume; and (iii) steady state conditions ($dC_X/dt=0$), taking into account the definition of dilution rate (D = F/V), the Equation (1) can be simplified as follows:

$\mu = D$

D is the reciprocal of the residence time (τ), which is defined as the average time that a fluid element spends inside the bioreactor (Richmond 2007; Fernandes *et al*. 2015).

Given this equivalence, by changing the residence time, a different growth rate can be imposed on the culture. Typically, once a transient period, roughly

three/four times the value of the residence time, has elapsed, a state of equilibrium is attained. During this state, nutrient consumption, biomass concentration and composition remain stable until there is a change in experimental conditions. At that point, a new transient period is observed, followed by the establishment of a new equilibrium (Trentin *et al*. 2021; 2023).

The principal advantage of cultivating microalgae in a continuous system is its capacity to maintain consistent conditions within the reactor over time, thereby ensuring successful large-scale production (Trentin *et al*. 2021). This is primarily attributed to higher volumetric productivity, stable product quality, reduced labour demands, and decreased operational expenses. Nevertheless, a drawback of this approach could be the heightened complexity of the system (Vale *et al*. 2020).

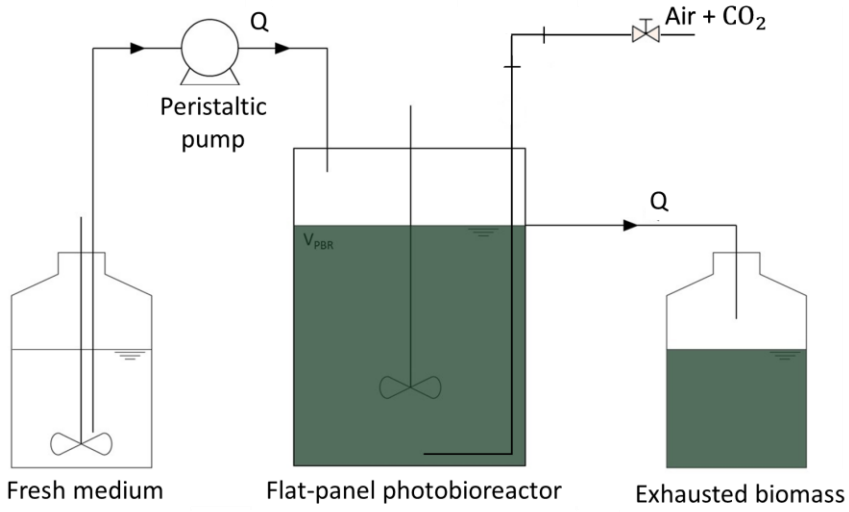

Fig. 1.4 Experimental set-up of a continuous experiment

1.5 Cultivation systems: photobioreactors

The systems usually employed for the cultivation of microalgae include both open system (such as open ponds, raceway ponds, scrubbers) and closed system, also

known as photobioreactors (PBRs) (including flat plate and tubular photobioreactors) (Ahmad *et al*. 2021).

On an industrial scale, microalgae are typically cultivated in open systems due to the low capital and operational costs, with the disadvantage of limited control of reaction conditions and potential contamination from harmful microorganisms. On the other hand, photobioreactors offer a closed culture environment, and are therefore widely accepted and used due to higher yield of biomass and product, better control of culturing conditions and growth parameters and contamination avoidance. However, this comes with the main drawback of high cost (Wang, Lan, and Horsman 2012; Vale *et al*. 2020; Benner *et al*. 2022).

Numerous photobioreactor designs have been developed, with the most prevalent types including flat plate, tubular, and column PBRs (Richmond 2007; Wang, Lan, and Horsman 2012). Alongside these more traditional photobioreactors, there are also less conventional alternatives with innovative designs, such as the CellDEG© photobioreactor (Chanquia, Vernet, and Kara 2022).

1.5.1 Vertical column photobioreactors

Vertical column photobioreactors are simple and economic systems consisting of cylindrical shaped vessels equipped with a gas sparger situated at the bottom. This transforms the incoming gas or air into small bubbles, serving as the driving force for mixing, facilitating the mass transfer of CO_2, and eliminating the O_2 generated during photosynthesis. To regulate the speed and size of the gas bubbles dispersed in the microalgae suspension, compressors and gas flow metres are combined with controllers. The air introduced at the bottom can either have an atmospheric composition or be sterilised air enriched with carbon dioxide (Richmond 2007; Ugwu, Aoyagi, and Uchiyama 2008; Wang, Lan, and Horsman 2012).

Vertical column photobioreactors can be further categorised into bubble column reactors or airlift reactors based on their flow pattern (Ahmad *et al*. 2021).

Bubble column PBRs (with working volumes typically ranging from 1 to 10 L) (Fig. 1.5) offer many advantages, including good high and mass transfer and low operating and maintenance costs due to the absence of moving parts. This type of PBRs is commonly used in research, but they can also serve as pre-culture devices (Ugwu, Aoyagi, and Uchiyama 2008; Ahmad *et al*. 2021; Benner *et al*. 2022).
Bubble column PBRs are typically illuminated using either fluorescent tubes or LED lamps. The incident light intensity decreases from the surface towards the centre of the cylindrical bubble column, potentially resulting in light-limited microalgae growth at the centre and photoinhibition effects near the surface. Therefore, an alternative approach involves internal illumination of the reactor, which results in enhanced light penetration capabilities and improved light distribution (Ahmad *et al*. 2021; Benner *et al*. 2022).
The incident light intensities typically employed in bubble column photobioreactors range from 15 to 220 µmol m^{-2} s^{-1}. Bubble column photobioreactors are commonly made of transparent materials when external illumination is employed. Typical materials include plastics like polyvinyl chloride or plexiglass, as well as glass. Both plastic options are cost-effective. Glass, on the other hand, is highly durable and is the only material that permits thermal sterilisation. Temperature control is achieved through a transparent double jacket surrounding the bubble column, or by placing the bubble photobioreactor inside an incubator (Ugwu, Aoyagi, and Uchiyama 2008; Benner *et al*. 2022).

Air lift PBRs are designed on the principle that the cylindrical vessel is divided in interconnecting zones. The inner tube, known as the gas riser or upcomer, allows the gas mixture to flow upward to the surface from the sparger. While in the outer portion, referred to as the downcomer, the medium flows downward and circulates back into the riser. Air lift PBRs can be further categorised into draft tube airlift PBR and split column airlift PBR (Fig. 1.5).

Undoubtedly, one of the primary benefits of an airlift PBR lies in its exceptional mixing capabilities. This facilitates effective exposure of cells to light radiation, even with a relatively large column diameter and high cell density (Wang, Lan, and Horsman 2012; Ahmad *et al*. 2021).

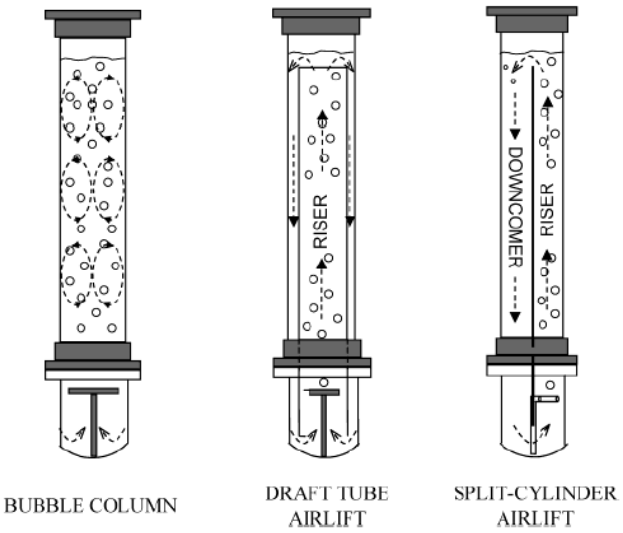

Fig. 1.5 Configurations of bubble column and airlift PBR (Wang *et al*., 2012)

1.5.2 Flat panel photobioreactors

Flat panel photobioreactors are closed systems characterised by a high illuminated surface to volume ratio (Fig. 1.6); this leads to efficient utilisation of light and minimisation of dark zones in the microalgae suspension. Flat panel PBRs consist of two joined plates whose thickness determines the surface area/volume ratio and the length of the light path. Generally, the shorter the light path, or thickness, the higher the optimal cell density (OCD) and biomass productivity (Wang, Lan, and Horsman 2012; Ahmad *et al*. 2021).

Common materials used for the plates include plastics such as plexiglass, polyvinyl chloride or polycarbonate and glass. Stainless steel frames are typically employed to support the transparent plates (Ugwu, Aoyagi, and Uchiyama 2008; Wang, Lan, and Horsman 2012; Benner *et al*. 2022).

Similarly to bubble column PBRs, flat plates can be employed as airlift photobioreactors with separated regions, one of which is aerated. The aeration is allowed through spargers, tubes, or membranes to promote mixing. In terms of illumination, LED lights are commonly used to illuminate flat panel photobioreactors. Typically, light intensities ranging between 80 and 400 µmol m^{-2} s^{-1} are applied. To maintain temperature control, transparent double jackets are utilised as heat exchangers, or alternatively, flat plate photobioreactors are immersed in water baths. In the case of smaller flat plate photobioreactors, they can be placed within temperature-controlled incubators (Zuccaro *et al*. 2020; Benner *et al*. 2022).

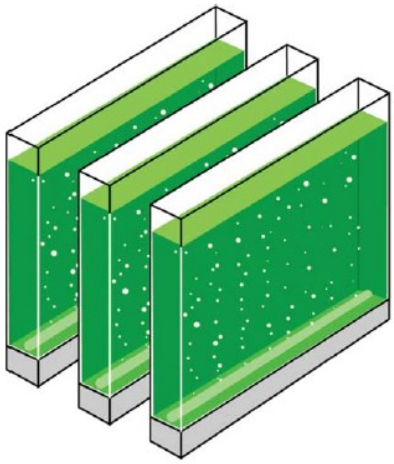

Fig. 1.6 Flat panel photobioreactors (Takenaka and Yamaguchi 2014)

1.5.3 Tubular photobioreactors

Tubular photobioreactors (Fig. 1.7) typically consist of two sections interconnected by pumps. The first section is the tubular component or the reactor where the microalgae are cultivated. In this part, the diameter of the tubes, which is generally 0.1 m or less, is optimised to maximise sunlight capture by the microalgae suspension. The second section is the degasser unit, employed for gas removal and facilitating circulation and mixing within the microalgae culture. Tubular photobioreactors have demonstrated their utility in various

operational modes, including semi-batch, batch, turbido-static, and continuous, establishing them as one of the most reliable types of photobioreactors for scaling up due to enhanced control. Tubular PBRs may have different orientations including horizontal, inclined, vertical arrangements (Wang, Lan, and Horsman 2012; Ahmad *et al*. 2021; Benner *et al*. 2022).

The design can also be scaled up to industrial capacities easily thanks to their modular construction approach. Various designs have been developed to enhance efficient light capture, with the most common ones including serpentine bioreactors, manifold bioreactors, which connect tubes of the solar receiver at both ends to two manifolds responsible for gas exchange and distribution, and helical bioreactors which consist of small flexible tubes that surround a frame structure (Benner *et al*. 2022).

Aeration and mixing of the cultures in tubular photobioreactors are commonly achieved using either air-pump systems or airlift systems. Controlling culture temperatures in many tubular photobioreactors can be a challenging task. While it is possible to equip them with thermostats to uphold the desired culture temperature, this approach can prove to be costly and complex to implement effectively. Additionally, it's important to acknowledge that cell adhesion to the walls of the tubes is a common occurrence in tubular photobioreactors (Ugwu, Aoyagi, and Uchiyama 2008).

Temperature, pH and oxygen concentration can be monitored at various points along the tube, depending on the nature of the experiment (Benner *et al*. 2022).

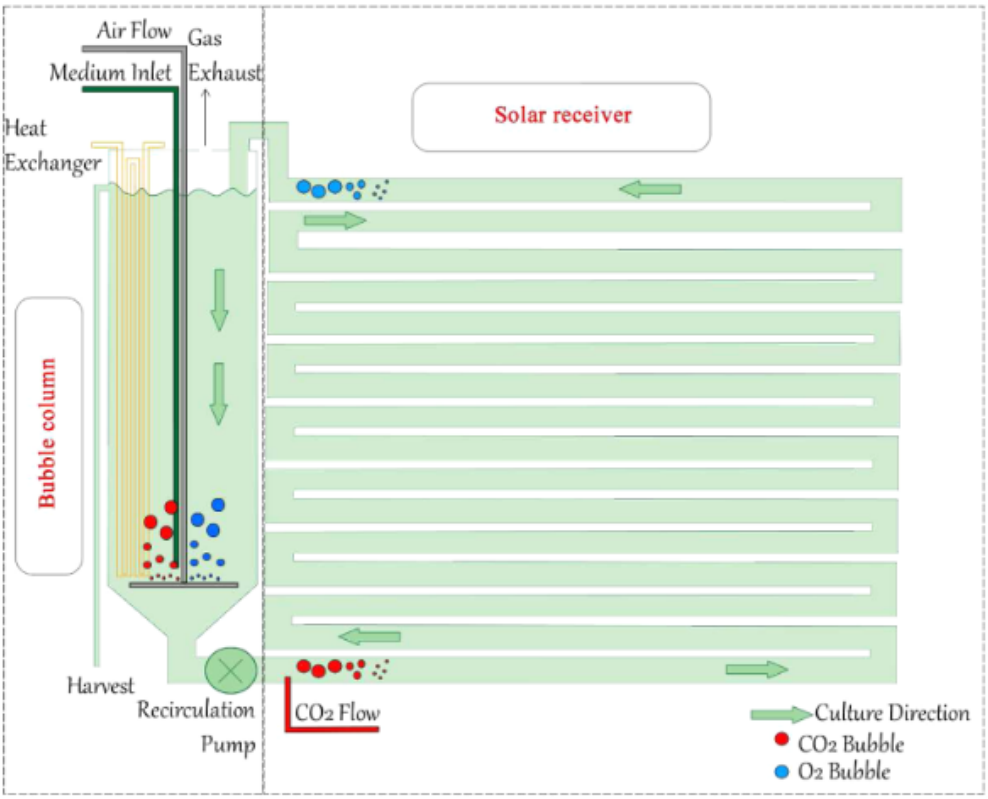

Fig. 1.7 Tubular PBR scheme (Fernández *et al*., 2014)

1.5.4 CellDEG© system

The CellDEG© system (CellDEG GmbH, Berlin, Germany) provides patented membrane photobioreactors characterised by high-density cultivation (HDC) technology, as it enables high cell densities and high biomass productivity in photoautotrophic cultures for biomass or bioproduct production at research and preparative scales (Lippi *et al*. 2018). This efficiency is achieved through the unique design of the photobioreactors. The cultivation system consists of detachable culture vessels, available in various culture volumes, connected via a CO_2-permeable polypropylene hydrophobic membrane to a dedicated CO_2 compartment. Here, the CO_2 concentration (typically 1-10%) is maintained either by a carbonate buffer (for volumes up to 150 ml) or controlled CO_2 injection (for volumes exceeding 150 ml). On the other hand, the vessel, also referred to as cultivator, holds the liquid culture and a turbulent gas phase, allowing oxygen release through diffusion via the outlet filter in the cap. This spatial separation

ensures a consistent supply of CO_2 to the culture, preventing CO_2 loss to the atmosphere and averting oxygen accumulation (Fig. 1.8) (Dienst *et al*. 2020; Chanquia, Vernet, and Kara 2022). High density cultivation in these photobioreactors is further facilitated by optimal light penetration and vigorous turbulent mixing. Specifically, the orbital shakers ensure minimal shearing stress to the cells, enabling rapid bubble-free mass transfer of CO_2 into the bulk culture. The CO_2 partial pressure in the bottom compartment, as well as the light intensity, is controlled by a growth control unit (GCU) (Lippi *et al*. 2018).

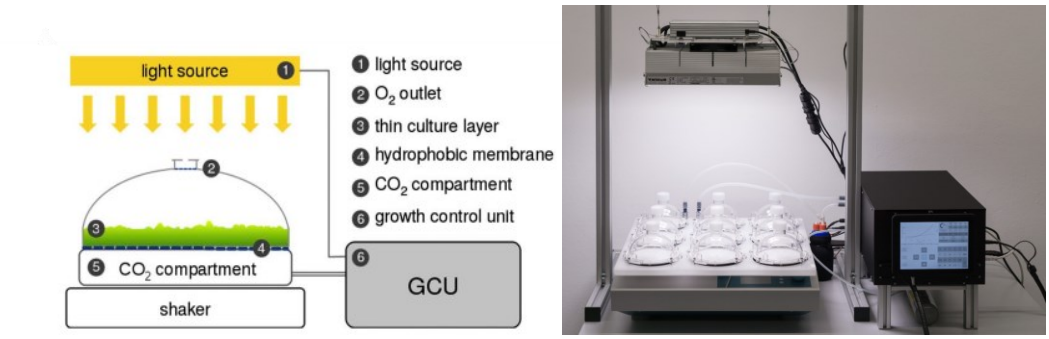

Fig. 1.8 The CellDEG© photobioreactor configuration (Lippi *et al*., 2018)

1.6 *Chromochloris zofingiensis*

1.6.1 Biological insights

Chromochloris zofingiensis is a unicellular non-motile freshwater Chlorophyte. Initially isolated and described by Dönz in 1934 as *Chlorella zofingiensis*, its taxonomic classification underwent several revisions. Ultimately, it was assigned to the genus *Chromochloris* by Fucíková and Lewis in 2012 (Reichelt *et al*. 2021; Zhang *et al*. 2021). In terms of morphology, this eukaryotic microorganism is characterised by spherical or oval cells, whose diameter varies from 2 to 15 μm depending on conditions and growth stages, and is surrounded by a rigid cell wall, composed mainly of glucose and mannose, which tends to thicken under stress conditions (Zhang *et al*. 2021; Wood *et al*. 2022). The life cycle is simple, involving three phases: growth, ripening, and division. Specifically, *Chromochloris zofingiensis* is a haploid organism that reproduces asexually through multiple fission in a consecutive pattern. This process involves multiple occurrences of DNA replication and nuclear division before the actual cell division takes place, resulting in the formation of polynuclear cells. Upon the rupture of the parental cell wall, autospores (up to 64) are spontaneously released (Figure 1.9) (Roth *et al*. 2017).

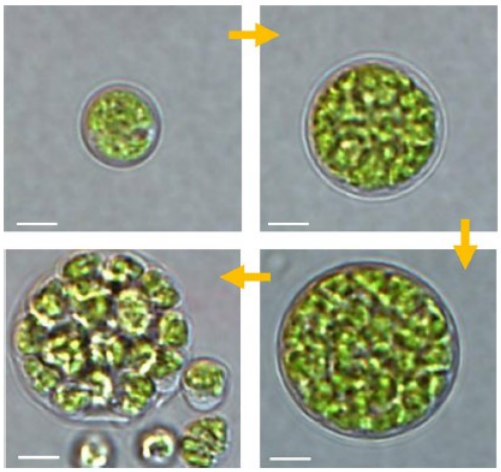

Figure 1.9 Light microscope image of *Chromochloris zofingiensis* cells under different growth stages. Bar, 2 µm (Zhang *et al*., 2021)

Observations using a transmission electron microscope reveal that under favourable growth conditions, *C. zofingiensis* cells appear green, with a cup-shaped chloroplast in which starch is abundant in scattered granules. Positioned peripherally in the cytoplasm, the chloroplast occupies approximately 12–50% of the cell volume, while the nucleus is somewhat centrally located. Mitochondria appear in an ovoid shape and are closely associated with the chloroplast. Additionally, lipid bodies are observed peripherally within the cell. In contrast, stress conditions harshly impair the cell structure of *C. zofingiensis*, whose cells turn orange due to the induction of secondary carotenoids. Under such conditions, lipid bodies may accumulate and merge to form a thick layer surrounding the shrunken chloroplast, which exhibits decreased starch levels (Figure 1.10; 1.11) (Liu *et al*. 2014; Wood *et al*. 2022).

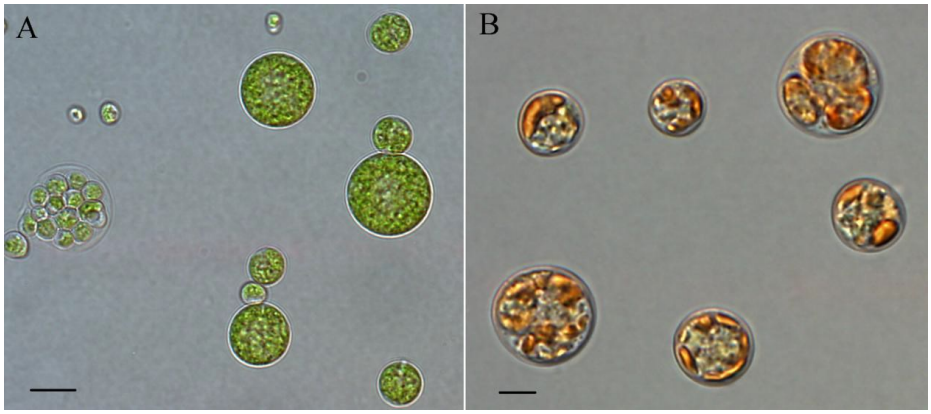

Figure 1.10 Light microscope image of *Chromochloris zofingiensis* cells under favourable (A) and stress (B) conditions. Bars, 5 µm (Liu *et al*., 2014)

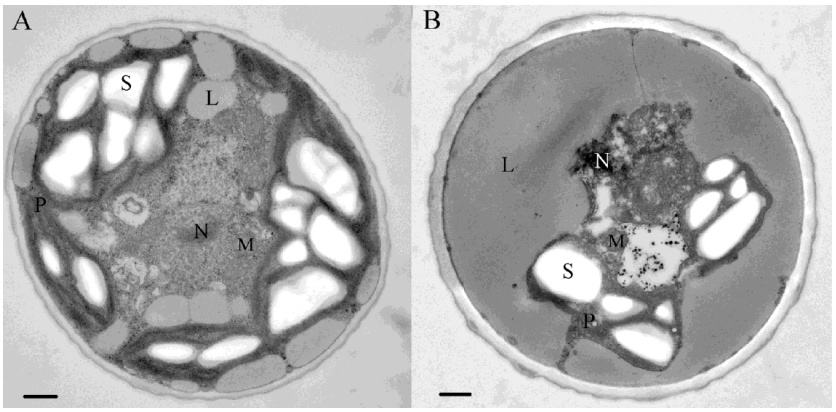

Figure 1.11 The ultrastructure of *C. zofingiensis* cells under favourable (A) and stress (B) conditions. Bars, 0.5 µm;·L, lipid body; N, nucleus; M, mitochondria; P, plastid; S, starch granule (Liu *et al*., 2014)

1.6.2 *C. zofingiensis* as a candidate producer of carotenoids and lipids

Chromochloris zofingiensis has attracted the interest of the scientific community due to its advantageous features, as it exhibits rapid and robust growth, being able to achieve high cell densities under photoautotrophic, heterotrophic and mixotrophic conditions (Zhang *et al*. 2021). But most importantly, this microorganism accumulates high value-added compounds such as lipids and secondary carotenoids simultaneously under stress-inducing conditions such as high light, limitation of nutrients, or high salinity (Liu *et al*. 2016; Wood *et al*. 2022). Specifically, under favourable growth conditions, algae primarily contain polar membrane lipids with a minimal level of triacylglycerides (TAGs), the most energy-dense storage lipids. On the other hand, upon stress conditions, algae slow down growth and accumulate TAGs as a carbon and energy reservoir. In a similar manner, specific stress conditions trigger the synthesis of keto-carotenoids (or secondary carotenoids) in certain green algae, including echinenone, canthaxanthin, adonirubin, adonixanthin, astaxanthin, and keto-lutein. These pigments are usually found outside of the chloroplast, in cytoplasmic lipid droplets (LDs). Notably, astaxanthin among the secondary carotenoids exhibits the strongest antioxidant activity (Zhang *et al*. 2021).

The coordinated and simultaneous accumulation of lipids and astaxanthin in lipid droplets makes *Chromochloris zofingiensis* an ideal candidate for the coproduction of these high-value added compounds, also resulting in an attractive target for biorefinery applications (Liu *et al*. 2016; Wood *et al*. 2022). A biorefinery is defined as a combined facility where downstream processes are integrated to produce a minimum of three distinct products from a sole source of biomass (Vanthoor-Koopmans *et al*. 2013; Chandrasekhar *et al*. 2022). The coproduction of multiple compounds not only enhances the value of biomass, lowering production costs and thus improving the cost-effectiveness of the cultivation process, but also promotes sustainable practices, reduces waste, and contributes to addressing the increasing demands for food, water, and energy. Additionally, the availability of more products increases production resilience against fluctuations in market value

and consumer demand. Additional proposed biorefinery outputs from *C. zofingiensis* include a broad range of value-added compounds, such as carotenoids like canthaxanthin, β-carotene, and lutein, diverse lipids, carbohydrates such as starch, and also proteins or amino acids. The Figure 1.12 shows all the potential products and applications of the components extracted from *Chromochloris zofingiensis* (Zhang *et al*. 2021; Wood *et al*. 2022).

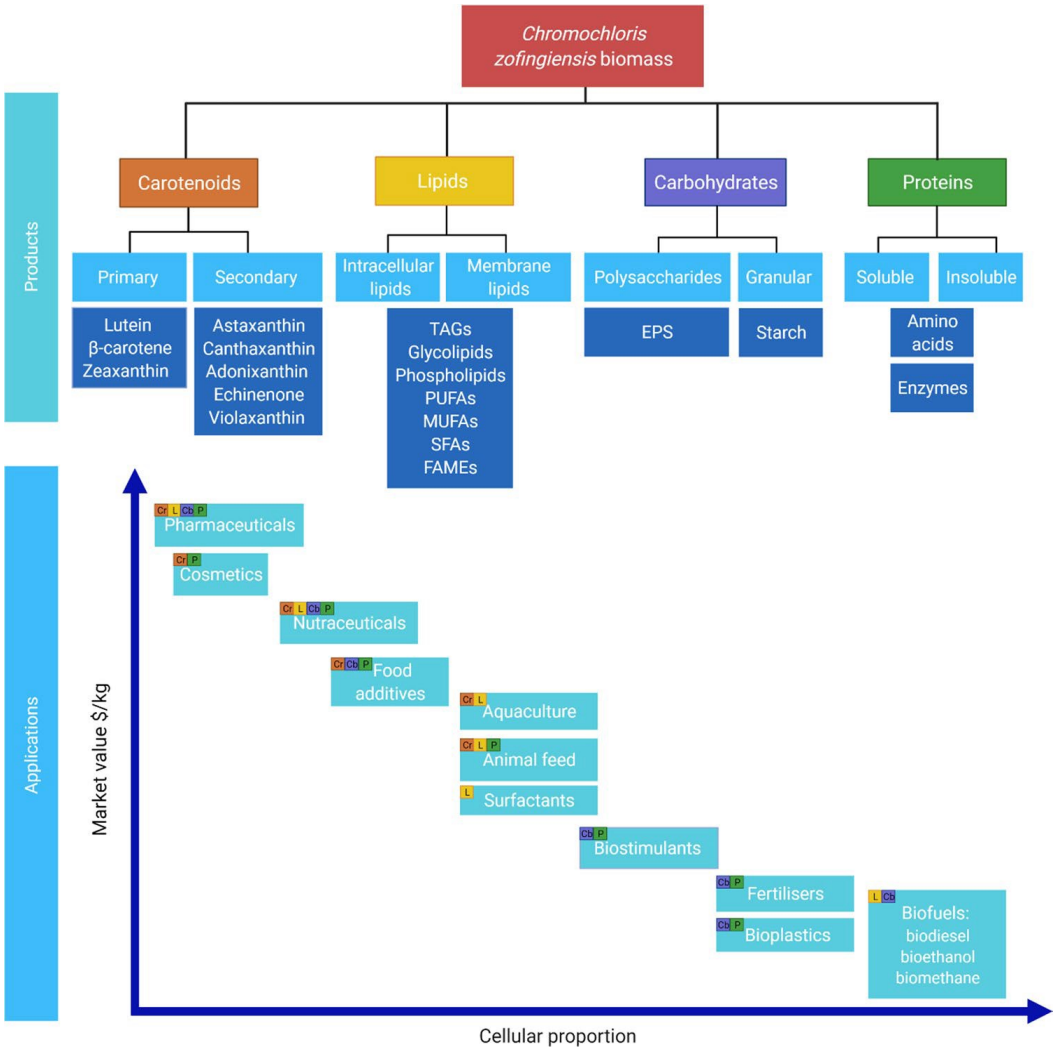

Figure 1.12 Potential products and applications of extracted components from *C. zofingiensis*. The coloured squares represent the products that can be used for each application (Wood *et al*., 2022)

1.7 Astaxanthin

Astaxanthin (3,3-dihydroxy-β,β-carotene-4,4-dione) is an orange-red coloured ketocarotenoid derived from canthaxanthin. It possesses both hydroxyl and ketone functional groups (Figure 1.13) (Gateau *et al*. 2017).

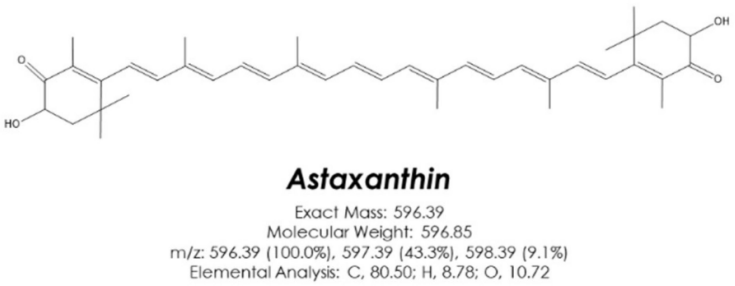

Figure 1.13 Chemical structure of astaxanthin (Villaró et al. 2021)

Astaxanthin finds wide-ranging applications across various industries, including feed, food, cosmetics, nutraceuticals, and pharmaceuticals. This is primarily due to its potent pigmentation capabilities and robust antioxidative properties (Gateau *et al*. 2017; Reichelt *et al*. 2021; Khoo *et al*. 2019). Moreover, numerous studies have highlighted its diverse health benefits for humans, such as reducing DNA damage, safeguarding eye and skin cells from UV-light-induced oxidative stress, mitigating inflammation by neutralising reactive oxygen species (ROS), enhancing the immune system through increased antibody production and T-cell count, and contributing to heart health by modulating LDL and HDL cholesterol levels (Liu *et al*. 2014). These exceptional properties of natural astaxanthin are among the primary reasons for its high value in the market which ranges from $6000 to $7150 per kg. The commercial market for astaxanthin is poised for significant growth and is estimated to reach a substantial $3.4 billion by the year 2027 (Nair *et al*. 2023). Astaxanthin can be obtained through either natural sources or synthetic production methods (Khoo et al. 2019). In nature, this compound is synthesised and accumulated to a considerable extent in certain green algae (*Haematococcus pluvialis*, *Chromochloris zofingiensis* and *Chlorococcum* sp.), some fungi (most notably in the red yeast *Xanthophyllomyces dendrorhous*, previously known as

Phaffia rhodozyma), and bacteria (such as the marine bacterium *Agrobacterium aurantiacum*), among others (Gateau *et al*. 2017; Nair *et al*. 2023).

Presently, synthetic production dominates the astaxanthin market, accounting for 95% of the production. This dominance is attributed to the prohibitively high production costs of naturally derived astaxanthin from *H. pluvialis*, which range from $2500 to $7000 per kilogram, compared to the $1000 per kilogram cost of synthetic production (Wood *et al*. 2022). Nevertheless, the complex synthesis process of synthetic astaxanthin involves the utilisation of petrochemical resources as raw materials. As a result, synthetic astaxanthin has not been approved for direct human consumption and is only used as an additive and pigment for fish feed purposes (Khoo *et al*. 2019; Nair *et al*. 2023). On the other hand, synthetic and natural astaxanthin differ in stereochemistry and structure. Natural astaxanthin not only presents a different ratio of stereoisomers, but is also commonly encountered as mono-esterified or di-esterified compounds with fatty acids, unlike synthetic astaxanthin which is typically found in its free form. This esterification of astaxanthin contributes to its inherent stability, rendering it less susceptible to oxidation (Liu *et al*. 2014; Wood *et al*. 2022). Several works have also indicated that the antioxidant activity of natural astaxanthin is significantly higher than the synthetic astaxanthin and other bio-compounds such as vitamin C, β-carotene, canthaxanthin, zeaxanthin, lutein and α-tocopherol (Khoo *et al*. 2019; Wood *et al*. 2022).

Nowadays, only natural astaxanthin is considered safe for human use (GRAS – generally recognized as safe) and consumption and has been approved by the European Commission to be commercialised as a bioproduct (Khoo *et al*. 2019; Nair *et al*. 2023). In order to make natural astaxanthin production cost-effective, various strategies and techniques need to be employed to increase astaxanthin yields and reduce production costs. In this context, microalgae are considered one of the most sustainable and ecological platforms for natural astaxanthin production (Gateau *et al*. 2017; Khoo *et al*. 2019; Reichelt *et al*. 2021). Currently, *H. pluvialis* is the primary natural producer of astaxanthin (about 4% of dry weight) and it is also the sole natural source of astaxanthin approved by the Food and Drug

Administration (FDA) for human nutrition (Gateau *et al*. 2017; Wood *et al*. 2022; Nair *et al*. 2023). However, the cultivation of *H. pluvialis* does present certain challenges, including complex life-cycle, slow growth rates, low biomass yields, susceptibility to contamination and high light requirements (Liu *et al*. 2014; Nair *et al*. 2023; Wood *et al*. 2023). The green alga *Chromochloris zofingiensis* has recently gained attention as a promising alternative for large-scale astaxanthin production. This is due to its above-mentioned advantageous characteristics, including rapid growth, resilience to contamination and challenging environmental conditions, and the ability to accumulate astaxanthin even when grown heterotrophically using glucose as the sole carbon and energy source (Liu *et al*. 2014). Although the highest astaxanthin content achieved in *Chromochloris zofingiensis* (13.1 mg per gram of dry weight) is still lower than that of *Haematococcus pluvialis* (> 40 mg per gram of dry weight), the overall astaxanthin yield (~194.5 mg per litre) and productivity (~9.9 mg per litre per day) for *C. zofingiensis* are comparable to, and in some cases even exceed, those of *H. pluvialis* (Zhang *et al*. 2021).

1.8 Aim of the thesis

In a context of a rapidly growing population and the consequent rise in demand for food, microalgae are increasingly emerging as an alternative and sustainable food solution with proven nutritional values and health benefits. Specifically, the chlorophyte *Chromochloris zofingiensis* is progressively gaining the attention of the scientific community, as it exhibits several features that make its application highly advantageous for biotechnological purposes. These characteristics encompass rapid growth, trophic flexibility and simultaneous synthesis of high amounts of triglycerides and secondary carotenoids, including the antioxidant valuable compound astaxanthin, in response to certain stress-inducing conditions (e.g. nitrogen limitation, salt stress, high light).

The purpose of this thesis work, carried out partly at the Technical University of Dresden and partly at the University of Padova, is to deepen the culture conditions effect on the production of high-value compounds such as carotenoids, specifically astaxanthin, and lipids. This was accomplished by growing *Chromochloris zofingiensis* under photoautotrophic conditions employing various types of photobioreactors and different cultivation strategies. In order to study the effect of nitrogen limitation itself and the combined effect of nitrogen limitation and salinity stress on the biomass growth and carotenoid and lipid production, *Chromochloris zofingiensis* was initially cultivated in a 200-L pilot-scale reactor manipulated in batch mode, following a two-stage cultivation strategy. This consisted in a first phase in which the microalga was cultivated under normal growth conditions to obtain maximum biomass yield, which was followed by a second phase where a stressor was applied. Subsequently, to comprehensively investigate the effect of these two types of stressors in a smaller and more controlled scale, further experiments were carried out in flat-plate photobioreactors operated in continuous mode. Finally, in order to accurately assess the effect of different stresses, and in order to find the optimal combination of stressors that results in maximising carotenoid and lipid production in *Chromochloris zofingiensis*, a Design of Experiment (DoE) statistical approach was applied to the CellDEG© high-density cultivation system.

Chapter 2: Materials and Methods

2.1 Algal strain and cultivation conditions

Chromochloris zofingiensis SAG 211-14 (Fig. 2.1) was purchased from the Culture Collection of Algae at Göttingen University (SAG, Germany) and maintained at 26°C in a 100 ml Erlenmeyer flask containing Bristol Modified Medium (BM Medium), with orbital shaking at 150 rpm and a light intensity of 50 µmol m^{-2} s^{-1} (16:8 light:dark cycle).

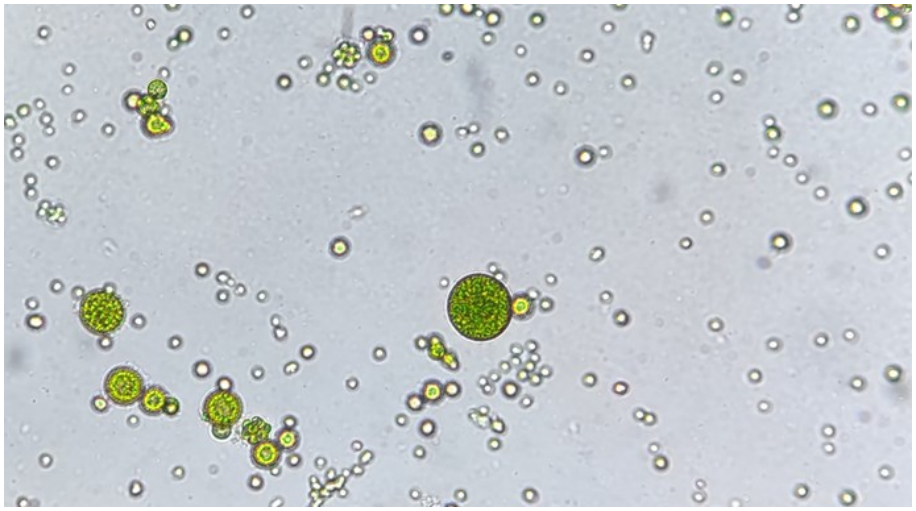

Fig. 2.1 Light microscope image of *Chromochloris zofingiensis*

The detailed composition of the BM medium (Ip, Wong, and Chen 2004) is shown in Table 2.1. For continuous experiments, the nutrient concentrations were doubled (BM**) to avoid the algae growth constraining while nitrate concentration was adjusted according to the experimental plan.

Tab. 2.1 Composition of BM medium (BM*) and doubled BM medium (BM**)

	Component	BM*	BM**
Nitrates (g L^{-1})	$NaNO_3$	0,75	1,5
Phosphates (g L^{-1})	KH_2PO_4	0,175	0,35
	K_2HPO_4	0,075	0,15
Mineral salts (g L^{-1})	$MgSO_4 \cdot 7H_2O$	0,075	0,15
	$CaCl_2 \cdot 2H_2O$	0,025	0,05
	NaCl	0,025	0,05
	$FeCl_3$	0,005	0,01
Trace elements (mg L^{-1})	$ZnSO_4 \cdot 7H_2O$	0,287	0,574
	$MnSO_4 \cdot H2O$	0,169	0,338
	H_3BO_3	0,061	0,122
	$CuSO_4 \cdot 5H_2O$	0,0025	0,005
	$(NH_4)_6Mo_7O_{24} \cdot 7H_2O$	0,00124	0,00248

Batch experiments were performed with commercial fertilizer as a growth medium, namely FERTY® 2 fertilizer (Planta Fertilizer GmbH, Germany) with a final concentration of 0,5 g L^{-1}, supplemented with 0,5 g L^{-1} $NaNO_3$ and 0,025 g L^{-1} $CaCl_2 \cdot 2H_2O$. The final medium composition with FERTY® 2 is shown in Table 2.2.

Tab. 2.2: Medium composition with 0,5 g L^{-1} of FERTY® 2

Composition	Concentration (g L^{-1})
N (as $NaNO_3$)	0.0147
P (as P_2O_5)	0.0154
K (as K_2O)	0.1368
Mg (as MgO)	0.0144
Fe (as DTPA)	0.002

2.2 Cultivation systems

2.2.1 Bubble column cultivation

Bubble column photobioreactors with a working volume of 800 mL (DURAN® GLS 80® Double Walled Bottle Wide Mouth, DWK Life Sciences GmbH, Germany) were utilised as pre-culture systems for the cultivation of *Chromochloris zofingiensis* (Fig. 2.2). A combination of blue and red light was provided continuously by a LED panel set at 80 µmol m^{-2} s^{-1}. Mixing was guaranteed by the bubbling of atmospheric air (gas flow rate of 20-30 L h^{-1}) in association with a magnetic stirrer located at the bottom of the reactor. Additionally, these systems were equipped with a double jacket for temperature control, kept constant at 25°C, and a humidification system for the inlet gas phase to reduce evaporation (DURAN® Gas Washing Bottle, DWK Life Sciences GmbH, Germany).

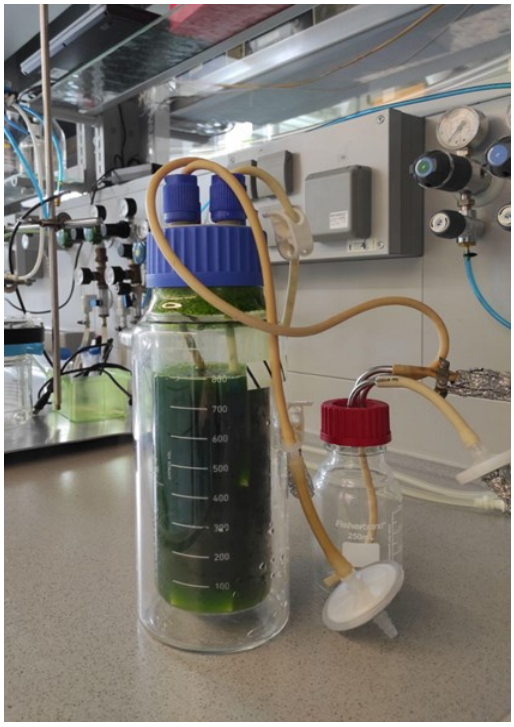

Fig 2.2 Bubble column PBR employed as pre-culture system at the University of Dresden (DWK Life Sciences GmbH, Germany)

2.2.2 Pilot-scale cultivation in a 200 L tubular PBR

The pilot-scale cultivation of *Chromochloris zofingiensis* was carried out photoautotrophically in a serpentine tubular photobioreactor with a working volume of 200 L (Fig. 2.3) under monitored conditions of pH, temperature, light intensity and dissolved oxygen.

The reactor consisted of two components: a tubular component or illuminated section where the microalga actually grew and a degassing unit for oxygen removal and mixing. The tubular component was made of transparent PVC tubes with a diameter of 0,065 m (Georg Fischer DEKA GmbH, Germany), connected by U-bends to form a loop configuration to achieve a total horizontal length of 2,7 m and a height of 1,98 m. LED lights were placed on the upper side of the wall of each tube, and could be modulated in colour and intensity. During the experiment, a white light was provided, and its intensity was set at 100 and 200 µmol m^{-2} s^{-1} during standard and stress-inducing cultivation, respectively.

The microalgal culture was continuously re-circulated by an airlift system with a flow rate of 10 L min^{-1}, while atmospheric air was injected to the inlet of the tubular component by means of a compressor. The reactor was additionally supplied with sensors for the measurement of turbidity, temperature, pH, dissolved oxygen concentration and light intensity with detection intervals of 1 minute. However, it should be mentioned that since there was no heat exchanger, the system temperature was subject to fluctuations depending on the temperature of the room, and ranged between 25 and 28°C.

Specifically, the cultivation of *Chromochloris zofingiensis* in the pilot-scale system was achieved by scaling up the cultivation of the alga first in 800 ml bubble column PBRs and then in a tubular serpentine PBR with a working volume of 25 L.

The complete system was designed and built by PUEVIT GmbH (Dresden, Germany), whereas the control and data acquisition was carried out by the Department of Process Control Systems of the University of Dresden.

Fig. 2.3 200 L tubular PBR located at the university of Dresden designed by PUEVIT (PUEVIT GmbH, Dresden, Germany)

Chromochloris zofingiensis was cultivated following an adaptation to the two-stage cultivation approach with the aim of investigating carotenoid and lipid production under varying culture conditions. This strategy consists of a first phase in which the microalga is cultivated in a nutrient-rich medium with optimal light intensity in order to accumulate biomass, followed by a second phase in which a stress condition is applied to boost carotenoid and lipid production (Minyuk *et al*. 2017; Ahmad *et al*. 2021). In this case, two types of stresses were investigated: nitrogen limitation and salinity stress. Specifically, this approach involved a first phase of biomass accumulation, under which the reactor was manipulated in batch mode under a light intensity of 100 µmol m^{-2} s^{-1}. This step was followed by a second phase of stress application consisting of nitrogen limitation, and a further phase of stress application consisting of nitrogen limitation in combination with salinity stress. During the stress phase, the light intensity was increased to 200 µmol m^{-2} s^{-1}, and a semi-continuous approach with a dilution rate of 0,05 day^{-1} was applied. This strategy involves periodic partial harvesting of the biomass from the reactor with subsequent replacement with fresh medium (Yin *et al*. 2020). This approach approximates the continuous cultivation mode, with the main difference

that in the latter case the fresh medium is constantly introduced into the culture at a rate corresponding to the removal of the exhausted biomass (Fernandes *et al*. 2015; Vale *et al*. 2020). The operating conditions for the pilot-scale cultivation are shown in Table 2.3.

Tab 2.3 Operating conditions for the cultivation of *C. zofingiensis* in the 200-L photobioreactor

	Medium composition		
Condition	**Cultivation time**	**N (mg L^{-1})**	**NaCl (g L^{-1})**
Standard growth	19 days	80	\
Nitrogen limitation	19 days	9	\
Nitrogen limitation and Salinity stress	13 days	9	15

2.2.3 Flat-plate photobioreactors cultivation

The experiments in continuous mode were performed by cultivating *Chromochloris zofingiensis* photoautotrophically in vertical flat-plate polycarbonate photobioreactors with a working volume of 160 mL, a thickness of 2 cm and an illuminated area of 80 cm^2 (Fig. 2.4). Fresh medium was constantly introduced into the culture at the same flow rate (Q) corresponding to the removal of exhausted biomass, using a multichannel peristaltic pump (205S/CA, Watson-Marlow Fluid Technology Group), thus keeping the volume of the reactor (V_{PBR}) constant. Continuous illumination was provided by a white LED lamp set at 120 µmol m^{-2} s^{-1}. Mixing was achieved through a magnetic stirrer at the bottom of the reactor and bubbling of a 1 L h^{-1} CO_2 air (5% v/v) mixture, approximating the system to a Continuous Stirred Tank Reactor (CSTR).

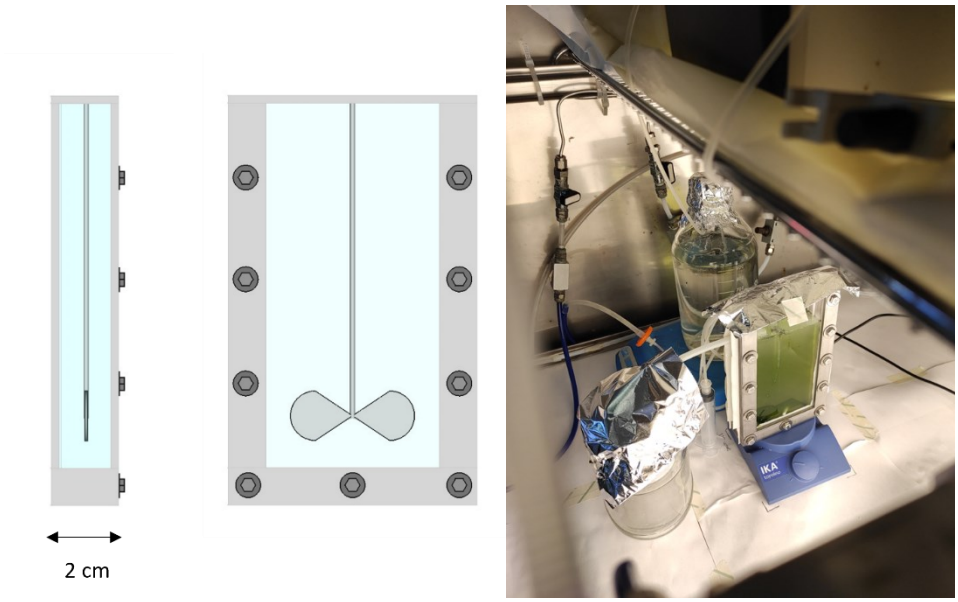

Fig. 2.4 Experimental setup of the flat-plate photobioreactor employed for continuous experiments with *Chromochloris zofingiensis*

The primary objective of implementing continuous cultivation for *Chromochloris zofingiensis* was to investigate the effect of nitrogen limitation and salinity stress on carotenoid and lipid production in a smaller and more controlled scale. To study the influence of the mentioned variables, the "one-factor-at-a-time" method was used, meaning the effect of the variable in question is evaluated by keeping the other variables fixed.

The effect of sodium chloride was first evaluated, keeping residence time, light intensity, and the inlet nitrogen concentration constant. Subsequently, the impact of the inlet nitrogen concentration in the medium was investigated, while maintaining the other variables fixed, as can be observed in Table 2.4. The residence time (τ) and the incident light intensity (I_0) were kept constant at 2 d and 120 µmol m^{-2} s^{-1}, respectively. Sodium chloride concentrations were varied between 0 and 15 g L^{-1}. Inlet nitrogen concentrations were varied modifying the concentration of sodium nitrate ($NaNO_3$) in the cultivation medium.

Tab. 2.4 Summary of operating conditions in continuous experiments with *Chromochloris zofingiensis*

Medium	Inlet nitrogen concentration (mg L^{-1})	Residence time (τ) (d)	Incident light intensity (I_0) (µmol photons m^{-2} s^{-1})	NaCl (g L^{-1})
BM $NaNO_3$ 2X**	246	2	120	0
BM $NaNO_3$ 2X**	246	2	120	15
BM $NaNO_3$ 1X**	123	2	120	15
BM $NaNO_3$ 0,5X**	61,5	2	120	15

2.2.4 CellDEG© cultivation

The cultivation of *Chromochloris zofingiensis* in the CellDEG© system took place in HD100 cultivators with a working volume of 150 ml under photoautotrophic conditions (Fig. 2.5) following a two-stage cultivation strategy in batch mode. The first phase of the cultivation was carried out under rich-nutrient conditions, while the second one was conducted under stress-inducing conditions. In the latter case, three different types of stresses were investigated: nitrogen limitation, salinity stress and high light intensity. A Design of Experiment (DoE) approach was applied in order to evaluate the effect of these variables alone or in combination on carotenoid production by *C. zofingiensis*, with the purpose of finding the optimal combination to maximise their production. The cultivators were supplied with 2% CO_2 enriched air and constantly shaken at 150 rpm on an orbital shaker (Edmund Bühler GmbH, Germany) (30 min in one direction and 1 min in the opposite direction). Light was provided continuously by a white LED lamp (LED KE 308, DH Licht, Germany).

In detail, the nutrient-rich phase was performed with an initial biomass concentration of OD_{750} equal to 1. This phase lasted 5 days, with an initial light intensity of 120 µmol m^{-2} s^{-1}, which was set at 240 µmol m^{-2} s^{-1} after two days. When the OD_{750} increased to 5, the stress phase was induced: biomass was harvested, pooled and resuspended in proper medium accordingly to the stress needed with a 6-day duration.

Fig 2.5 Picture of HD100 cultivators provided by the CellDEG© system

Tab. 2.5 Design of Experiment performed by Design Expert 13

Run	Experiments	Factor 1 (NaCl g L^{-1})	Factor 2 ($NaNO_3$ g L^{-1})	Factor 3 (Light intensity µmol m^{-2} s^{-1})
1	2	5	1	400
	3	30	1	400
	12	15	0	400
	5	15	2	400
2	6	15	1	700
	8	15	1	700
	9	5	0	700
	10	5	2	700
	11	15	1	700
	13	30	0	700
	14	15	1	700
	16	30	2	700
3	1	15	0	1000
	4	30	1	1000
	15	15	2	1000
	7	5	1	1000

2.3 Biomass estimation

Several methods were used for the quantification of biomass. The optical density at 750 nm was determined by measurement with a spectrophotometer (GENESYS 150 UV/VIS-spectrophotometer, ThermoFisher, U.S.A.). In all cultivation systems considered, the dry weight content was determined gravimetrically. Pre-dried (60°C for at least 4 h) and pre-weighed glass fibre filters (ROTILABO®, Type: CR260; diameter 47 mm, Carl Roth, Germany) were used for the gravimetric method. Filters were rinsed with deionised water pre and post filtering. The biomass on the filter paper discs was then dried in the oven at 60°C O/N and was subsequently cooled down to room temperature in a desiccator before weighing. The weight difference was then measured and the dry weight for each sample calculated based on the volume passed through the membrane filter.

In the pilot-scale experiment, freeze-drying method was additionally employed for biomass determination. The freeze-drying method was performed by collecting the biomass in pre-weighed 50 ml falcon tubes. The falcons were then subjected to a first centrifugation at 15000 rpm for 10 minutes, followed by pellet washing with deionised water and a second centrifugation under the same conditions as above. The pelleted biomass was stored at - 80°C, subsequently dried in a freeze-dryer (Beta 1-8 LSC basic freeze-drier, Martin Christ GmbH, Germany) and eventually weighed. Again, the weight difference was measured and the dry weight for each sample calculated based on the volume of biomass used.

For batch experiments, the specific growth rate (μ) (day^{-1}) in the exponential phase and the biomass productivity P_X (g L^{-1} day $^{-1}$) were calculated according to the following equations (Minyuk, Sidorov, and Solovchenko 2020):

$$\mu = \frac{\ln C_{X,1} - \ln C_{X,2}}{t_1 - t_0} \qquad \text{Eq.2.1}$$

$$P_X = \frac{C_{X,1} - C_{X,0}}{t_1 - t_0} \qquad \text{Eq.2.2}$$

where C_X is the biomass concentration (g L^{-1}) according to the dry weight and (t_1 – t_0) is the time interval considered (d). The latter refers only to the exponential phase for specific growth rate and to the whole batch experiment duration for biomass productivity.

In continuous experiments, where the system considered was approximated to a CSTR, the specific growth rate μ (d^{-1}) and the biomass productivity P_X (g L^{-1} d^{-1}) were calculated following the equations below (Trentin *et al*. 2023):

$$\mu = D = \frac{1}{\tau} = \frac{Q}{V_{PBR}} \quad \text{Eq. 2.3}$$

$$P_X = \frac{C_X}{\tau} \quad \text{Eq. 2.4}$$

where D is the dilution rate, which is the inverse of the residence time τ (d); C_X is the biomass concentration according to dry weight (g L^{-1}) measured at steady state.

2.4 Analytical measurements

2.4.1 Pigment extraction and analysis

Dimethyl sulfoxide (DMSO) (Carl Roth, Germany) was used as the extraction solvent on biomass samples stored at - 80°C and previously thawed. In detail, the procedure involved diluting the sample with water to obtain 1 mL of sample with OD_{750} between 0,3 and 0,7 in a 2 mL eppendorf (for samples with OD below 0,3, this step was skipped). This step was necessary to fall within the reading range of the spectrophotometer. The next step was to centrifuge the samples at 15000 rpm for 10 minutes, then discard the supernatant and resuspend the pellet in 1 mL of DMSO, then vortex, with subsequent passage to the thermoshaker (HLC Cooling-ThermoMixer MKR 13, DITABIS - Digital Biomedical Imaging Systems AG, Germany) at 70°C, 700 rpm for 10 minutes, followed by centrifugation under the conditions described above. The final step was to properly dilute the DMSO extract with DMSO and analyse the samples in the spectrophotometer (range between 350 and 800 nm).

The content of chlorophylls *a* and b (Chl *a*, Chl *b*), total carotenoids (Car) and astaxanthin (µg ml^{-1}) was determined by spectrophotometric measurement using GENESYS 150 UV/VIS-spectrophotometer (ThermoFisher, U.S.A.) and the equations given below (Wellburn 1994; Franke *et al*. 2022):

$$[Chl\ a] = 12{,}19\ [Abs_{665} - Abs_{750}] - 3{,}45\ [Abs_{649} - Abs_{750}] \quad \text{Eq. 2.5}$$

$$[Chl\ b] = 20{,}05\ [Abs_{649} - Abs_{750}] - 5{,}32\ [Abs_{665} - Abs_{750}] \quad \text{Eq. 2.6}$$

$$[Car] = \frac{(1000\ [Abs_{530} - Abs_{750}] - 2{,}14\ [Chl\ a] - 70{,}16\ [Chl\ b])}{220} \quad \text{Eq. 2.7}$$

The astaxanthin concentration was derived from the calibration curve, which was obtained with solutions of known concentrations of pure astaxanthin and is depicted in Fig. 2.6.

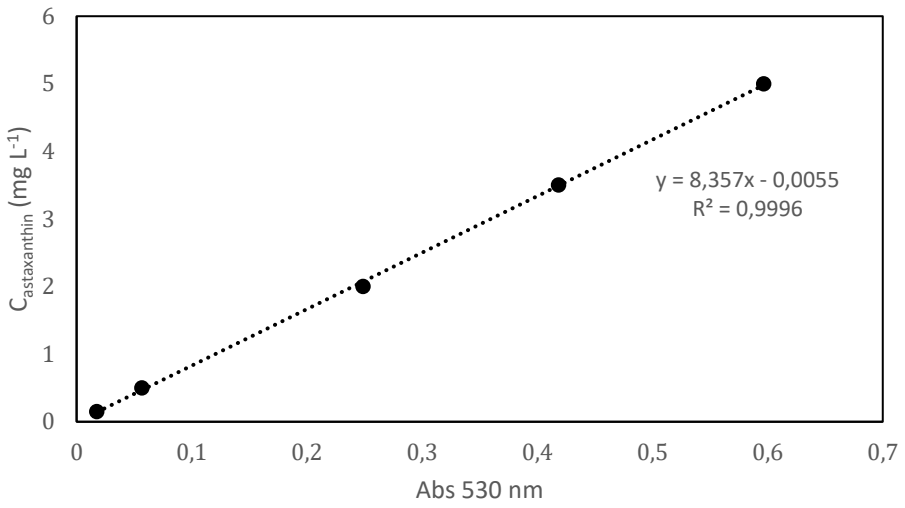

Fig. 2.6 Astaxanthin correlation curve

$$[Astaxanthin] = [Abs_{530} - Abs_{750}] * 8{,}357 - 0{,}0055 \quad \text{Eq 2.8}$$

2.4.2 Lipid extraction and analysis

Cell samples were harvested, washed and freeze-dried for lipid extraction and analysis. Lipid extraction was performed using the Soxhlet method. The Soxhlet method is one of the most traditional and commonly used techniques for extracting lipids in foods. This system presents mainly three compartments: flask, extraction chamber, and condenser (Fig. 2.7). The dried sample is placed in a porous thimble. Once the flask is heated, the solvent is evaporated and moved up to the condenser, where it is turned into liquid and collected into the extraction chamber containing the sample. As the solvent passes through the sample, it extracts the fats and transports them into the flask. At the end of the extraction, the solvent is evaporated, and the remaining lipid mass is measured and subjected to further analysis. The main drawback of this method is its laboriousness, as well as the use of dangerous, flammable and more expensive organic solvents (Hewavitharana *et al*. 2020).

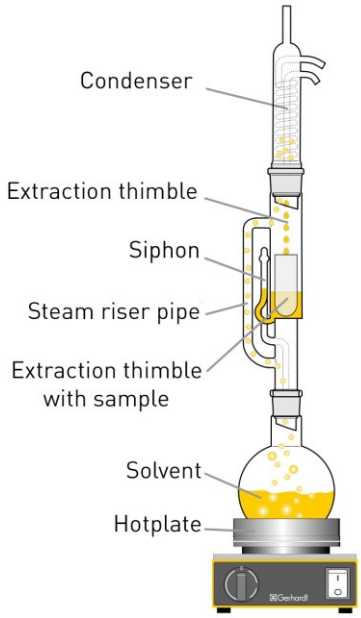

Fig. 2.7 Soxhlet extractor (Gerhardt, Germany)

The lipid analyses carried out with the Soxhlet extraction system were performed using the Soxtherm device (Gerhardt, Germany) and Petroleum Ether 40-60°C as the extraction solvent (VWR International, U.S.A.). The lipid extraction was preceded by an acid pretreatment using hydrochloric acid as solvent. In detail, the biomass was weighed into a 400 ml beaker, to which 100 ml of deionised water was added, stirring with a glass rod. The 25% HCl solution was then prepared and 100 ml of this solution was added to the sample. The beaker was placed on the heating plate at 200°C and covered with the glass plate: the boiling point was waited for, then the temperature was lowered until small bubbles appeared. After one hour, 100 ml of boiling water was added to the sample. For filtering the sample, a 2000 L Erlenmeyer flask and a cellulose filter (ROTILABO®, Type: 600P; diameter 185 mm, Carl Roth, Germany) were taken. The content of the beaker was added to the filter, and the filter was then rinsed with boiling water until the percolation water was completely neutral (verified by litmus paper). The filter was placed at 60°C O/N and subsequently used for the Soxhlet extraction.

The total lipid content, expressed in g per 100 g of biomass sample or in percentage, was determined as follows (Wood *et al*. 2023):

Total lipid content (%DW or $g_{lipids}/100g_X$) = $(W_2-W_1)/W_0 \times 100$ Eq. 2.9

where W_1 corresponds to the weight of the empty extraction flask (g), W_2 corresponds to the weight of the extraction flask containing the extracted lipid (g) and W_0 to the biomass weight of the analysed sample (g).

2.4.3 Pigment and lipid productivity

In continuous and semi-continuous experiments, the pigment and lipid productivity P_i (g L^{-1} d^{-1}) was calculated following the equation below (Borella, Sforza, and Bertucco 2021):

$$P_i = \frac{C_{i,out}}{\tau} \quad \text{Eq. 2.10}$$

where $C_{i,out}$ is the concentration (g L^{-1}) of the component i (e.g. pigment, lipid) at reactor outlet measured at steady state.

2.4.4 Total nitrogen analysis

Nitrogen concentration analysis on inlet medium, sample filtrates and within biomass was performed using the TOC-L equipped with TNM-L (Shimadzu Corporation, Kyoto, Japan). The samples were appropriately diluted to be within the calibration curve (5 µg L^{-1} - 100 mg L^{-1}).

This method is based on high-temperature combustion coupled with chemiluminescence detection. In detail, the samples containing nitrogen compounds undergo decomposition into nitrogen monoxide (NO) at 720°C through combustion. The thermoelectrically cooled and dehumidified NO gas flows through the chemiluminescence analyser, reacting with ozone to produce a

combination of nitrous oxide (NO_2) and excited nitrous oxide (NO_2*). When NO_2* reverts to its fundamental state, it emits radiation that is detected photo-electrically. The signal from the detector generates a peak that is proportional to the nitrogen concentration in the sample (Fig. 2.8).

The relative nitrate concentration can be derived using the molecular weights of N, NO_3 and $NaNO_3$. The consumption of nitrogen can be calculated through the difference between the nitrogen concentration in the inlet medium and the sample filtrates. On the other hand, biomass nitrogen content (q_N) is calculated as the ratio of nitrogen concentration within biomass by biomass concentration.

$$q_N = \frac{C_N}{C_X} \qquad \text{Eq. 2.11}$$

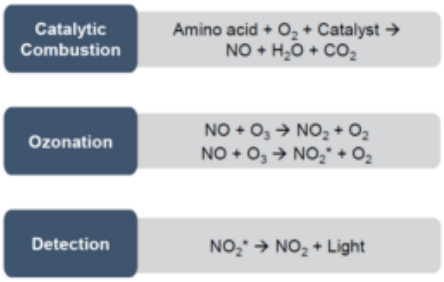

Fig. 2.8 Total nitrogen analysis reaction process

2.5 Statistical analysis

The statistical analyses of the data were performed using the MiniTab statistical package. One-way ANOVA was used to compare equal variances, by means of Tukey's method. The statistical significance was achieved when $p < 0,05$.

2.5.1 Design of Experiment

The Design of Experiment (DoE) statistical approach was applied to the CellDEG© high-density cultivation system. Usually, the most straightforward experimental procedure is carried out following the so-called "one-factor-at-a-time" approach, varying one variable at a time while keeping the others constant. However, this approach does not take into account the interactions between the variables and any effects of these on the response variable. The DoE, on the contrary, is a statistical approach that allows the simultaneous and systematic evaluation of multiple input variables or factors in order to determine the variables that have the most influence on the response variable, and in general to clarify the conditions that determine the optimal response values (Jankovic, Chaudhary, and Goia 2021). There is a variety of different DoEs that can be chosen depending on the type of investigation. Here, the DoE was performed using a Box-Behnken (BBD) experimental design. The Box-Behnken design provides an understanding of the system behaviour, revealing the type of connection between factor and response, and its optimization at the same time. It is similar to a Central Composite Design (CCD), but requires fewer experimental runs and is particularly suitable to use when several factors simultaneously exhibit extreme values (Jankovic, Chaudhary, and Goia 2021).

In detail, given sodium chloride (NaCl) concentration (g L^{-1}), sodium nitrate ($NaNO_3$) concentration (g L^{-1}), and light intensity (I_0) (µmol m^{-2} s^{-1}) as input factors and considering three levels for each factor, the software Design Expert 13 suggested an investigation plan including 16 experiments listed in Table 2.5 reported previously. Only the central point condition has been tested in replicates

(experiments 6, 8, 11, 14), according to the DoE approach, to estimate the pure error, not due to the input factors. Given the pure error, the software calculates the lack of fit, namely a statistical parameter representing the goodness of the model in describing the experimental dataset. Practically, the experiments were grouped according to light intensity and performed at the same time resulting in three different runs (Table 2.5).

Chapter 3: Pilot-scale cultivation in a 200-L tubular PBR

The pilot scale cultivation of *Chromochloris zofingiensis* was carried out in a 200-L tubular PBR following an adaptation to the two-stage cultivation approach with the aim of investigating carotenoid and lipid production under varying culture conditions. As a matter of fact, in *Chromochloris zofingiensis*, as in other carotenogenic microalgae, rapid cell division and the accumulation of reserve lipids and secondary carotenoids do not occur simultaneously. These processes take place at different stages of the life cycle and require significantly different cultivation conditions. According to the two-stage cultivation approach, it is possible to distinguish an initial so-called "green cell stage", corresponding to a phase in which there is an accumulation of biomass, followed by a phase referred to as "red cell stage", due to the generation of secondary carotenoids and simultaneous lipogenesis (Minyuk *et al*. 2017). Notably, this latter phase is induced by applying a stressor or a combination of stressors (e.g., elevated irradiance and essential nutrient deprivation). Specifically, in the pilot-scale reactor, two types of stress-inducing conditions were investigated: nitrogen limitation and salinity stress. In detail, the two-stage cultivation approach involved a first phase of biomass accumulation, followed by a second phase of stress application consisting of nitrogen limitation, and a further phase of stress application consisting of N-limitation in combination with salinity stress. The operating conditions for the pilot-scale cultivation are detailed in the Materials and Methods chapter in the section §2.2.2.

The results related to biomass growth, pigment and total lipid profiles will now be reported and briefly discussed.

3.1 Biomass growth in the pilot-scale

The growth of *Chromochloris zofingiensis* as dry weight (DW) and OD_{750} in response to different culture conditions has been examined and its trend is shown in Fig. 3.1. It can be observed that initially, under nutrient-rich conditions (N-replete medium), the biomass follows an exponential trend, with a specific growth rate (μmax) of 0,071 day^{-1}. Growth then decreases, once stress is applied by diluting the culture with N-depleted medium till the end of the cultivation. Starting from day 19, in fact, with a frequency of about 3 days, the semi-continuous cultivation method is applied, for which part of the content is removed from the reactor and replaced with fresh N-depleted medium. In detail, a significant drop in biomass concentration can be observed between days 19 and 20 ($p < 0,05$). This is supposedly due to the fact that on day 19, approximately 30% of the reactor volume was replaced with N-depleted medium. This drastic drop appears to be followed by a slight increase in biomass content, indicatively from day 20 to day 26. This recovery could be due to the remaining, albeit minimal, presence of nitrogen in the medium that was not fully consumed in the exponential growth phase. The nitrogen consumption was then investigated and presented in the next paragraph.

This decreasing trend of biomass concentration continues till the last applied stress phase, where nitrogen deficiency is combined with salinity stress. In fact, despite the initial slight decrease (days 38-41), the biomass concentration remains almost constant during the combined stress application.

From Fig. 3.1, it is also evident that the biomass trend is reflected by that of the optical density measured at 750 nm. It would seem, however, that the profile of OD_{750} is less pronounced than that of biomass. It should be emphasised here, that although spectrophotometry offers a simple and rapid approach to measure the cell concentration of unicellular microorganisms, this method face two major issues: it is limited to a low range of cellular concentrations (the absorbance should range between 0,1 and 0,8) to ensure linearity between the absorbance value and the cell density and it is additionally affected by the presence of non-cellular, scattering particulates, such as sodium chloride (B. Kell *et al*. 1990).

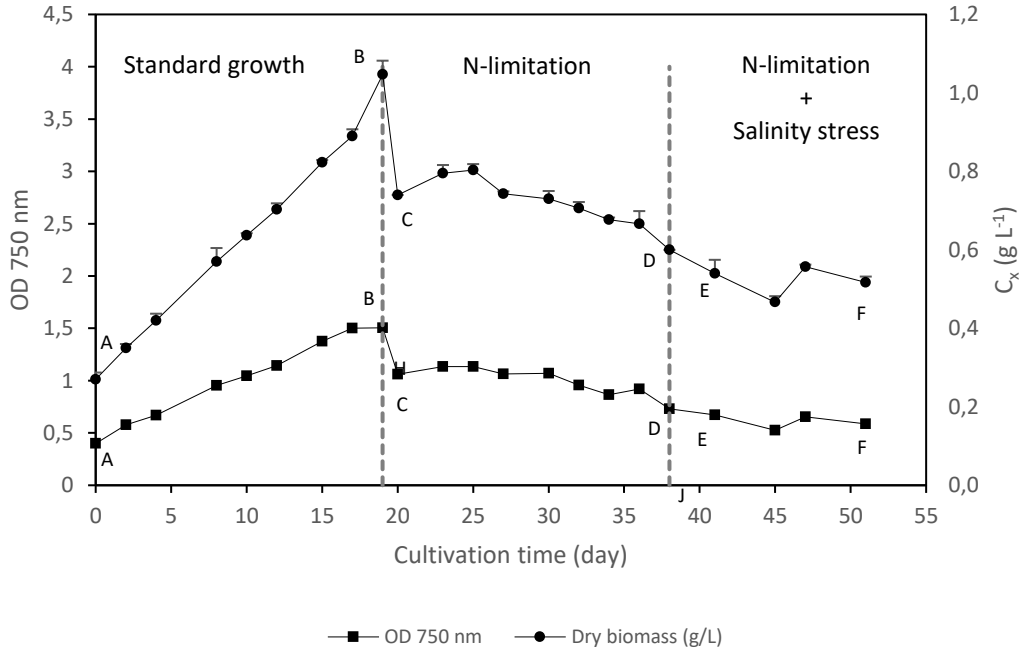

Fig. 3.1 Biomass concentration as dry weight (dots) and OD_{750} (squares) as a function of cultivation time (day). The data are expressed as mean ± SD (n = 3). Different letters indicate significant difference between data ($p < 0,05$), based on one-way ANOVA with post hoc Tukey's HSD test. Statistics refers to the same data set.

The decrease in the growth of *Chromochloris zofingiensis*, which is usually accompanied by an enlargement of cell size, is a normal consequence of the application of both N-limitation and salinity stress conditions and has been widely documented in the literature (Zhang *et al*. 2021). The algal growth is usually impaired by stressful conditions in a concentration-dependent manner: the higher the salt concentration, or the lower the nitrogen concentration, the lower the cell density and growth rate (Liu *et al*. 2016; Mao *et al*. 2020; Wood *et al*. 2023). This results are particularly evident under nitrogen starvation conditions (complete absence of nitrogen in the growth medium). The ideal trade-off, therefore, would be to find those conditions that allow a good production of the compound of interest, without significantly compromising the growth of the biomass, as reported in the work of Liu *et al*. (2016). In this work, similarly to the present study, a semi-continuous approach coupled with N-limitation strategy was applied. However, although the nitrogen concentration employed is similar (9 mg L^{-1} in the

present work versus 10 mg L^{-1} in their work), the dilution rate and consequently the residence time applied is different (20 d in the present work and 2 d in their work), and this could justify a low biomass productivity at the end of N-limitation phase in the present experiment. In this regard, it should be mentioned that the choice of the residence time employed was based on technical reasons related to the company's practice.

For what concerns the sodium chloride contribution, the salinity level employed in this experiment is equal to 15 g L^{-1}. This value seems to imply a slight, but not drastic decrease in biomass growth, in accordance with what reported in the work of (Mao *et al*. 2020) in the presence of a sodium chloride concentration of 0,2 M (approximately 12 g L^{-1}) and to what reported in the study by Kou *et al*. (2020) under the same sodium chloride concentration (0,25 M).

In any case, it should be pointed out that the exponential growth rate reported in this experiment (0,071 day^{-1}) turns out to be very low compared to those found in the literature in similar conditions (Wood *et al*. 2023), and this is probably due to the fact that no CO_2-enriched air was supplied to the culture. In the recent study by Wood *et al*. (2023), in particular, during the so-called green phase, corresponding to the accumulation of biomass (conducted in a 65-L PBR over a 15-day time period), a growth rate of approximately 0,154 day^{-1} was reported, which is almost twice as high as that obtained in this work. This was mainly attributable to the presence of efficient aeration/mixing coupled with CO_2 inputs. So, it appears that the protocol preliminary applied for this species is not the most suitable to increase productivity, and should be improved by managing the operative variables to avoid light and carbon limitation.

3.2 Nutrient consumption in the pilot-scale: nitrogen

The availability of nitrogen in the medium was experimentally determined along the days of cultivation. Initially, under standard growth conditions, the nitrogen profile exhibited an inverse relationship with biomass growth, as depicted in Figure 3.2, whereby as biomass increased, nitrogen availability in the medium decreased due to the consumption by the microalga for the growth. From the analysis, nitrogen resulted almost completely consumed at day 19. It reasonable that longer cultivation in such condition would have led to growth slow down and the achievement of the growth stationary phase. For this reason, on day 19, the first stress phase was applied. From this moment on, and throughout the duration of the stress phase, the nitrogen concentration in the medium remained relatively constant since no statistically significant differences have been highlighted ($p > 0,05$).

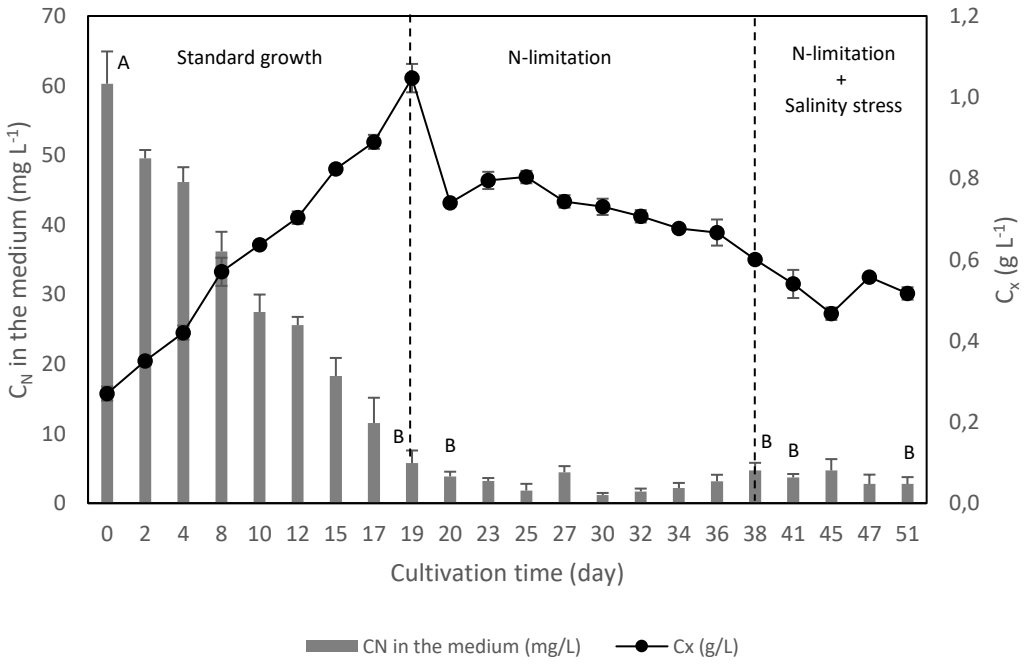

Fig. 3.2 Nitrogen content in the medium (supplied as sodium nitrate) and biomass concentration profile over cultivation time (day). Values are mean ± SD (n = 3). Different letters indicate significant difference ($p < 0,05$), based on one-way ANOVA with post hoc Tukey's HSD test.

3.3 Pigment profile in the pilot-scale

The pigments content was also evaluated during the cultivation to assess their accumulation according to the culture conditions.

In Figure 3.3, it can be appreciated that under standard growth conditions, the pigment profile of *Chromochloris zofingiensis* is dominated by chlorophyll *a* and, to a lesser extent, chlorophyll *b* (up to 22,425 ± 0,690 and 8,674 ± 0,251 mg g^{-1} DW, respectively), with the synthesis of only a small amount of total carotenoids (up to 5,637 ± 0,198 mg g^{-1} DW). Upon application of N-limitation condition, it is possible to notice that there is a marked decrease in chlorophyll *a* and *b*. However, this is not associated with a significant enhancement of carotenogenesis, which was actually induced only after the implementation of both types of stressors. At the end of the experiment, carotenoid content amounted to 7,478 ± 0,772 mg g^{-1} DW, while a further decrease in chlorophyll *a* and *b* content (7,520 ± 0,499 and 3,412 ± 0,338 mg g^{-1} DW) was also observed. The productivity of total carotenoids during the first stress phase is reported to be 0,167 mg L^{-1} d^{-1}, while it increased to 0,193 mg L^{-1} d^{-1} with the combined application of N-limitation and salinity stress to the culture.

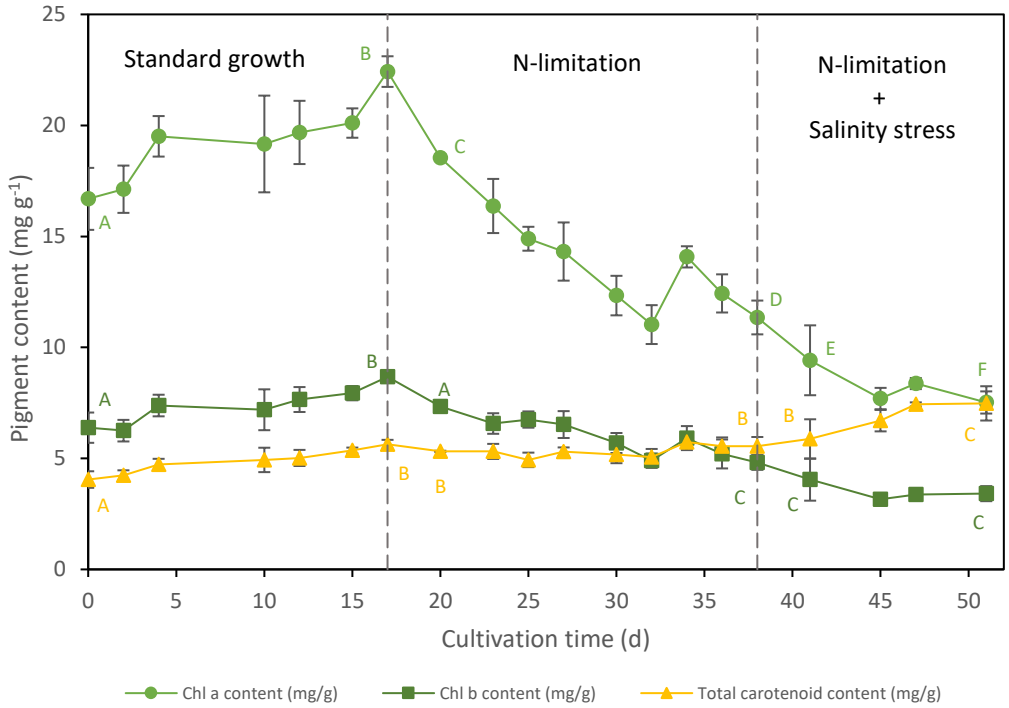

Fig. 3.3 Pigment content within biomass as a function of cultivation time (day). Values are mean ± SD (n = 3). Means that do not share a letter are significantly different. Statistics refers to the same data set.

Additionally, as a support of the increased carotenoid content because of stress application, the ratio of total carotenoids to chlorophylls (Car/Chl), which is considered an indicator of carotenogenesis as well as an index of stress response (Chen, Wei, and Pohnert 2017; Wood *et al*. 2023), has been calculated. Indeed, the Car/Chl ratio increased from an initial value of 18% to 34% at the end of the first stress phase, and then to 68% as a result of the second stress phase (Fig. 3.4).

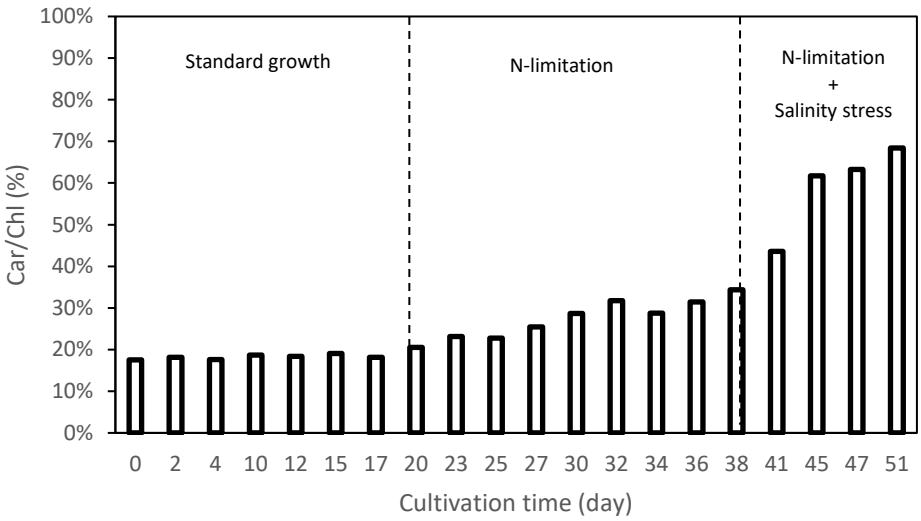

Fig. 3.4 Car/Chl ratio (%) as a function of cultivation time (day).

Furthermore, in Figure 3.5, it can be noticed how the variation in pigment content that occurred at different cultivation stage, reflected the shift in colour of the algal biomass.

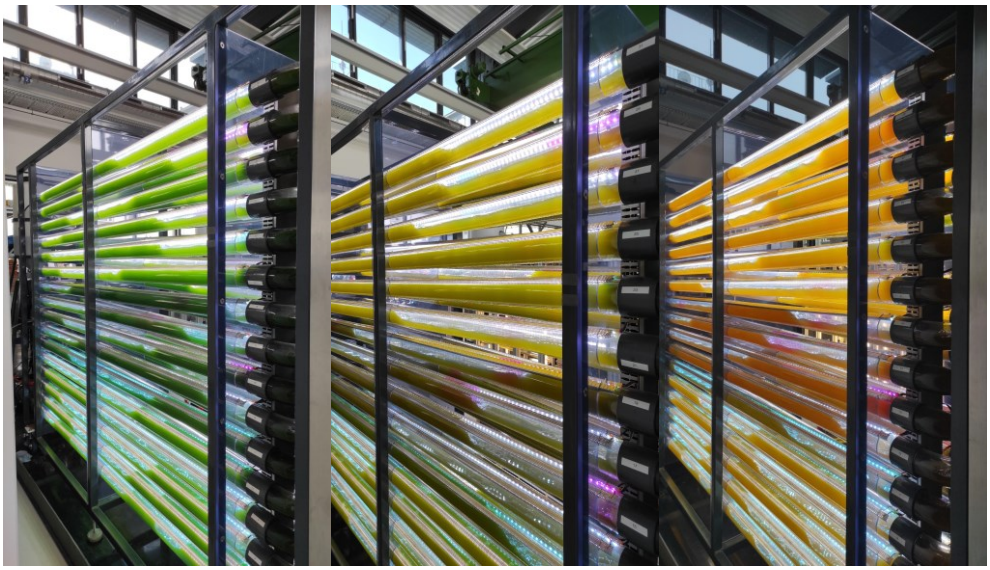

Fig. 3.5 Variation in the composition of photosynthetic pigments in *C. zofingiensis* under varying culture conditions.

3.3.1 Astaxanthin production in the pilot-scale

In addition to primary carotenoids, produced under normal, favourable growth conditions, some algae also synthesize keto-carotenoids, known as secondary carotenoids, such as echinenone, canthaxanthin, adonirubin, adonixanthin, astaxanthin and keto-lutein. Unlike primary carotenoids, secondary carotenoids are generated in large quantities only under particular stress conditions, playing a crucial role in safeguarding the cell against oxidative stress (Orosa *et al*. 2001; Minyuk *et al*. 2017; Zhang *et al*. 2021).

Since the main aim of this thesis is to evaluate the accumulation of the valuable ketocarotenoid astaxanthin following the application of various stress-inducing conditions, the astaxanthin content per dry weight has been measured and the productivity of the pigment calculated.

The Figure 3.6 illustrates in orange the trend of astaxanthin content as a function of time. It can be observed that there is a significant increase in astaxanthin content at the end of N-limitation phase, with a value of 2,443 ± 0,117 mg g^{-1} DW on day 38. While by the end of the second stress phase, represented by the combination of N-limitation and salinity stress, the astaxanthin content reaches 3,823 ± 0,278 mg g^{-1} DW. The Figure 3.6 also shows the trend in the relative abundance of astaxanthin on carotenoids, which at the very beginning of the experiment is around 35%, rises to 44% following the application of N-deficiency stress, and increases to 51% at the end of the combined stress phase. The productivity of astaxanthin during the first stress phase is reported to be 0,073 mg L^{-1} d^{-1}, while it increased to 0,099 mg L^{-1} d^{-1} with the combined application of N-limitation and salinity stress to the culture.

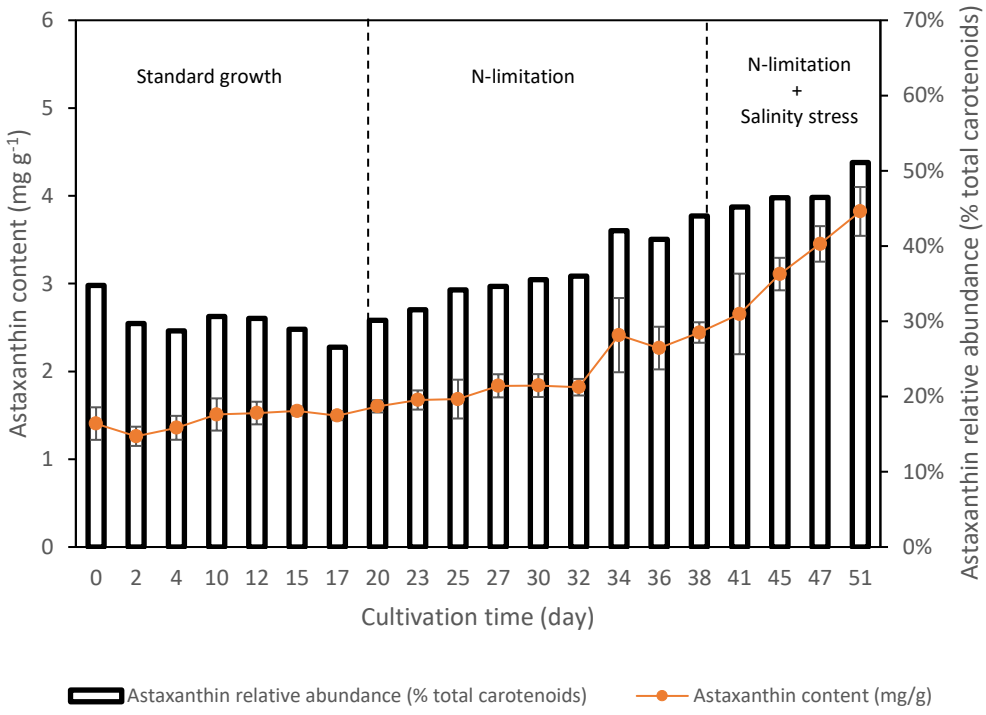

Fig 3.6 Astaxanthin content and astaxanthin relative abundance (% of total carotenoids) as a function of time (day).

The production of astaxanthin from photoautotrophic cultures of *C. zofingiensis* has been extensively investigated under various stress conditions, including nitrogen deprivation, high light, and salinity stress, contributing to a better understanding of the ketocarotenoid production (Liu *et al*. 2019; Zhang *et al*. 2021).

Looking specifically at the nitrogen limitation strategy (not in combination with salinity stress) applied in the present work, this included the use of a nitrogen concentration in the medium of approximately 9 mg L^{-1}. A similar nitrogen concentration (10 mg L^{-1}) as well as a semi-continuous cultivation approach are also reported in the previous work by (Liu *et al*. 2016). In their study, in contrast to this thesis work, the nitrogen concentration of 10 mg L^{-1} gave not only a higher intracellular astaxanthin content (3,2 mg g^{-1}), but also a high productivity of astaxanthin (3.3 mg L^{-1} day^{-1}). Nevertheless, it should be specified that both the reactor scale and the residence time used (2 d) in their work are not comparable to those used in this study.

Similarly, at the level of the combined stress phase, the final astaxanthin content, equal to 3,823 ± 0,278 mg g^{-1}, which is comparable to that obtained in the work of Mao *et al*. (2018) (3,9 mg g^{-1} DW), is not accompanied by consistently high productivity (0,099 mg L^{-1} d^{-1}). This is because, in general, when considering of optimising the yield of a particular compound by microalgal culture, such as astaxanthin may be, both the parameters of content of the compound and biomass growth must be taken into account (Del Campo *et al*. 2004). In this case, high pigment content is not coupled with biomass growth, but with a decrease in biomass, thus resulting in low pigment productivity. This evidence was also highlighted in the work of Orosa *et al*. (2001), who reported an astaxanthin content of 6,8 mg g^{-1} DW, following the combination of three stressors, specifically high light, N-starvation (no nitrogen at all) and salinity stress. There again, the high astaxanthin content did not go along with productivity, which was reduced due to impaired cell growth.

To date, beyond the already mentioned study of Orosa *et al*. (2001), there is a lack of information in the literature reporting *C. zofingiensis* cultivation under combined N-limitation and salinity stress conditions. Another work is the one by Vozelj Pia (Master thesis, 2023), in which laboratory-scale experiments were conducted with a nitrogen concentration in the medium of approximately 41 mg L^{-1} and a sodium chloride concentration of 0,2 M (about 12 g L^{-1}).

Therefore, the here presented master thesis represents the first work conducted on a 200-L pilot scale PBR to simultaneously analyse the combined effect of N-limitation and salinity stress on the accumulation of carotenoids and, specifically, astaxanthin.

The sodium chloride concentration of 0,2 M is considered to be the ideal salt concentration for astaxanthin accumulation in *C. zofingiensis* (Del Campo *et al*. 2004; Mao *et al*. 2020). Specifically, in the work of Mao *et al*. (2020), of the various salt concentrations tested, the most promising for astaxanthin accumulation proved to be 0,4 M NaCl (approximately 23 g L^{-1}). This concentration, however, consistently impaired biomass growth, thus resulting in lower astaxanthin productivity. Given these considerations, it was therefore plausible that the use of

an intermediate concentration between these two values, such as the one used in the present work, equal to 15 g L^{-1}, could result in a simultaneous increase in astaxanthin content and productivity. However, the result obtained, as already mentioned, is that of a high astaxanthin content that is not accompanied by an equally high productivity.

Further studies will therefore be required to elucidate the concentrations of nitrogen and sodium chloride needed to optimise astaxanthin content and productivity.

3.4 Lipid content profile in the pilot-scale

Considering that conditions inducing carotenogenesis can also induce lipogenesis, lipid content has been quantified to evaluate the potential application of the biorefinery approach. The latter would offer the possibility of extracting different products of interest, in this case carotenoids and lipids, from a single production system (Wood *et al*. 2022).

As depicted in Figure 3.7, the total lipid content increased progressively under nitrogen deficient conditions, reaching a value of about 14% on day 39, but it was only with the combined effect of nitrogen depletion and salinity stress that it considerably increased up to 25% per DW (day 51). This indicates that the combination of the two stressors appears to be more effective than N-limitation alone in stimulating the lipogenesis. It should be noted that the anomalous value found on day 23 is plausibly due to partial loss of the sample.

The productivity of lipid has also been calculated and is reported to be 0,042 mg L^{-1} d^{-1} at the end of the first stress phase, while it increased to 0,065 mg L^{-1} d^{-1} with the combined application of the two stressors.

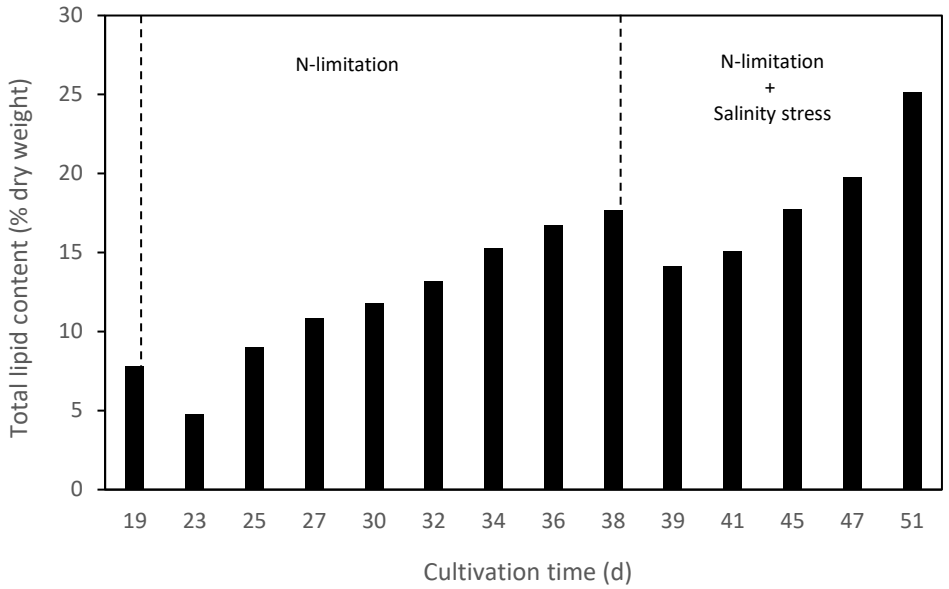

Fig. 3.7 Lipid content (% DW) in function of cultivation time (day). The statistic is not reported because the number of samples was not sufficiently high.

Oleaginous microalgae, named for their capacity to produce oil, are documented to store 30–70% of lipid content under conditions of nutrient starvation (Pal *et al*. 2019). Under normal growth conditions, algae predominantly synthesize components vital for biological membranes, such as membrane lipids, phospholipids, glycerol-phospholipids, and glycolipids, with low levels of neutral lipids, such as triglycerides (TAGs). Under growth-restricting conditions, on the contrary, algal cells absorb excess carbon but face impediments in cell division, shifting their lipid synthesis pathway to accumulate TAGs, used as a carbon and energy reservoir, at the expense of protein and starch (Liu *et al*. 2019; Pal *et al*. 2019). The accumulation of lipids in *C. zofingiensis* has been studied under various stress-inducing conditions, including limitation or starvation of nutrients, high light, salinity, and abnormal temperature (Zhang *et al*. 2021).

As pointed out in the work of Liu *et al*. (2016), the total lipid content responds differently depending on the culture conditions. In general, in the present work, the reported values in lipid content appear to be low compared to those found in the literature. Under standard autotrophic growth conditions, Liu *et al*. (2011) reported a total lipid content value of 25,8%, as opposed to this study, where it

amounts to 7,84%. In the following study from 2016, Liu *et al*. reported that under N-depletion conditions (no nitrogen supplied), there was a considerable increase in the total lipid content, which was found to be almost 50% after a 6-day batch cultivation. While in the present study amounts to 25%. Therefore, a plausible explanation for these strong contrasting values may be due to possible oxidation of the lipids, which were not properly treated during the extraction phase. Furthermore, since lipids were not characterised in the present study, it is difficult to make considerations in this regard. Similar to what has been advanced about astaxanthin content, the low lipid productivity found at the end of the two stress phases could be due to an excessive drop in biomass growth. In general, the assumptions that have been made about astaxanthin production also apply in the case of lipid production.

Chapter 4: Continuous experiments

The experiments conducted in continuous mode on flat-plate photobioreactors had as their prime purpose the detailed study of the effect of the two stressors applied to the pilot-scale reactor, namely nitrogen depletion and salinity stress, on the production of carotenoids and specifically astaxanthin. This, in order to identify which culture condition resulted in higher carotenoid content and productivity. Indeed, the continuous mode is associated with the possibility to maintain stable conditions within the reactor over time, assuring constant quantity and quality of the biomass produced, and consequently of the compound of interest (Trentin *et al*. 2021). Furthermore, the smaller scale ensures an easier and better management of factors such light availability, pH, temperature, CO_2 supply and O_2 release, all variables that are complex to control on large-scale cultivation (Benner *et al*. 2022). It should be also pointed out that, to date, the continuous cultivation strategy applied to *Chromochloris zofingiensis* is an area of research that is still unexplored, as there is a lack of reference scientific literature. In detail, the effect of the presence of sodium chloride and the influence of different nitrogen concentrations in the medium were investigated employing the "one-factor-at-a-time" approach. Specifically, an experimental residence time τ of 2,01 ± 0,12 d was applied, corresponding to a specific growth rate of 0,5 ± 0,03 d^{-1}, while a light intensity value of 120 µmol m^{-2} s^{-1} was set. This setup was established on the basis of batch experiments conducted previously at the University of Dresden (Lory Ascoli, Master thesis, 2023). The experimental conditions used to operate in continuous mode for *Chromochloris zofingiensis* are described in the Materials and Methods chapter in the section §2.2.3.

4.1 Study of the effect of sodium chloride concentration

With the aim of understanding the effect of sodium chloride presence on biomass growth and astaxanthin production, lab-scale experiments were conducted in continuous mode without or with NaCl in the medium. The latter was carried out by adding 15 g L^{-1} of NaCl in the medium, on the basis of the same sodium chloride concentration adopted on the pilot-scale reactor.

4.1.1 Biomass growth under salininity stress

The Figure 4.1 shows the steady-state biomass concentration and the biomass productivity upon changing the sodium chloride concentration employed. It is evident that under the two different NaCl concentrations tested, the biomass growth, as well the biomass productivity, remain practically unchanged ($p < 0,05$), demonstrating that a sodium chloride concentration of 15 g L^{-1} does not result in a biomass impairment.

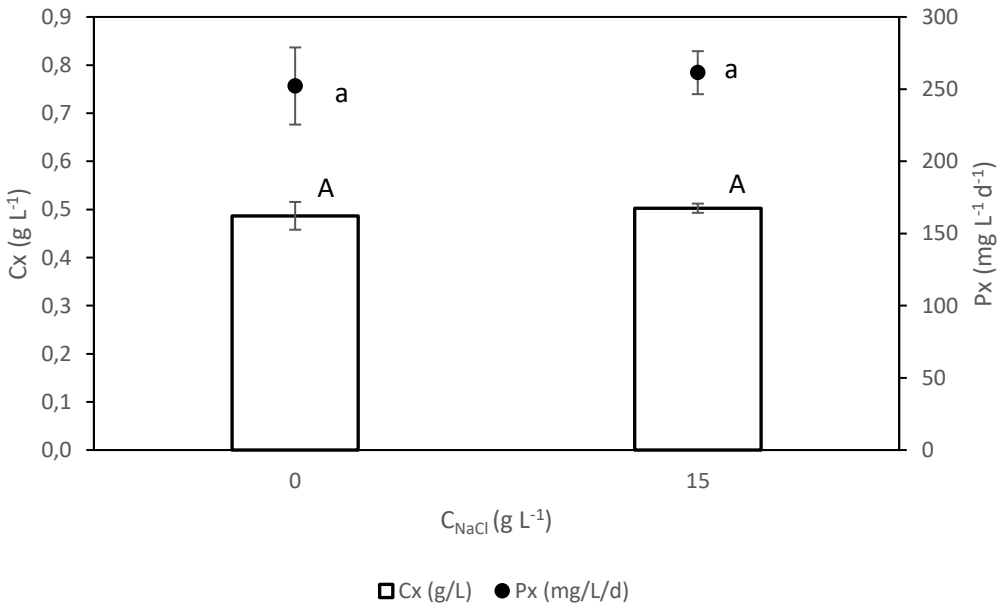

Fig. 4.1 Steady-state biomass concentration (bars; g L^{-1}) and productivity (dots; mg L^{-1} d^{-1}) in absence or presence (15 g L^{-1}) of sodium chloride in the medium. Values are mean ± SD (n = 3). Means that do not share a letter are significantly different. Statistics refers to the same data set.

This result differs from what was seen in the pilot scale PBR, where there was a slight but significant decrease in biomass growth. However, it is consistent with experiments conducted in batch mode with similar sodium chloride concentrations (approximately 12 g L^{-1}) (Mao *et al*. 2020). In this regard, it should be specified that the continuous cultivation strategy, by maintaining a constant exponential phase, allows a greater ability to withstand stresses.

4.1.2 Pigment and astaxanthin production under salinity stress

For what concerns the pigment profile, in Figure 4.2 it can be observed that the presence of 15 g L^{-1} of sodium chloride significantly increased ($p < 0,05$) the accumulation of total carotenoids, without inducing a consistent reduction in Chl *a*, nor in Chl *b* content. The latter, in fact, were kept constant at 0,67 ± 0,21% and 0,70 ± 0,09% for chlorophyll *a*, and 0,32 ± 0,11% and 0,18 ± 0,02% for chlorophyll *b*. This proves that the photosynthetic apparatus is not impaired by stress, as already seen in the biomass concentration which does not decrease.

The total carotenoid content on the other hand increased from 0,20 ± 0,06% to 0,37 ± 0,02% in the condition with 15 g L^{-1} of NaCl. Looking at the total carotenoid productivity, this amounts to 0,451 mg L^{-1} d^{-1} in the condition where no additional salt is provided and to 0,966 mg L^{-1} d^{-1} in the experiment where 15 g L^{-1} of NaCl is supplied. This shows that the increased carotenoid content is also accompanied by an increased carotenoid productivity. The fact that the productivity of carotenoids doubled is justified by the increased pigment content without a reduction in biomass growth due to the stress.

In addition, in both experiments, the ratio of total carotenoids to chlorophylls (Car/Chl) was calculated to be 20% for the experiment conducted without further salt addition and 42% for the experiment with 15 g L^{-1} NaCl, further demonstrating the increase in total carotenoid content following salt treatment.

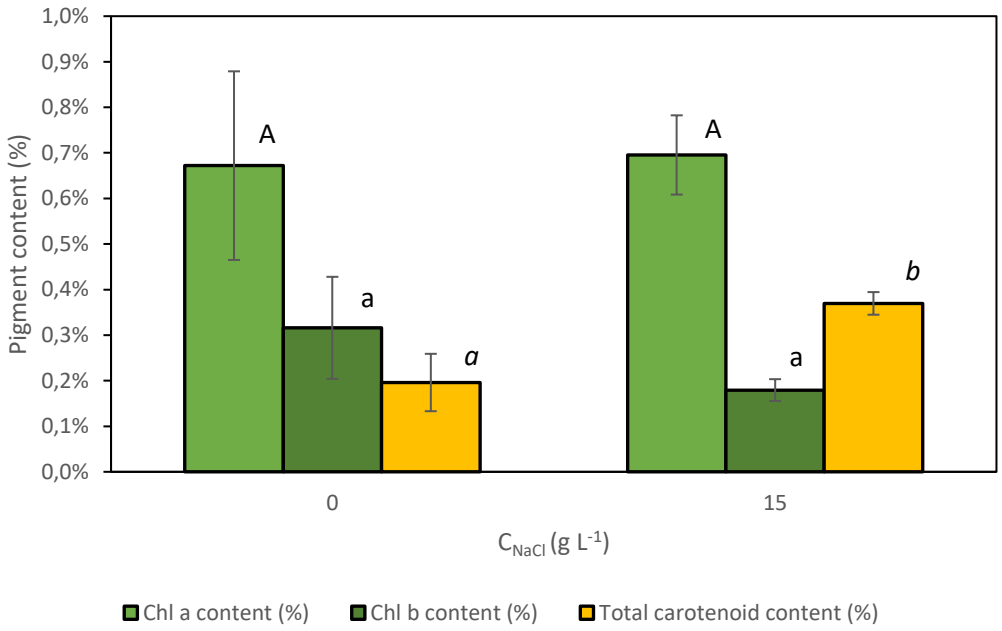

Fig. 4.2 Steady-state Chlorophyll *a*, Chlorophyll *b* and carotenoid content (% DW) in absence or presence (15 g L^{-1}) of sodium chloride. Values are mean ± SD (n = 3). Means that do not share a letter are significantly different. Statistics refers to the same data set.

With regard to astaxanthin, in the Figure 4.3 it is possible to observe the ketocarotenoid content and productivity. In line with what has already been shown in the previous graph, the condition corresponding to a salt concentration of 15 g L^{-1} determined an accumulation of the pigment, which is twice as high as in the condition where no additional salt is present. Again, the increase in astaxanthin content is reflected in an increased productivity, which rises from being 0,232 mg L^{-1} d^{-1} in the condition where no salt is provided, to 0,528 mg L^{-1} d^{-1} in the other one.

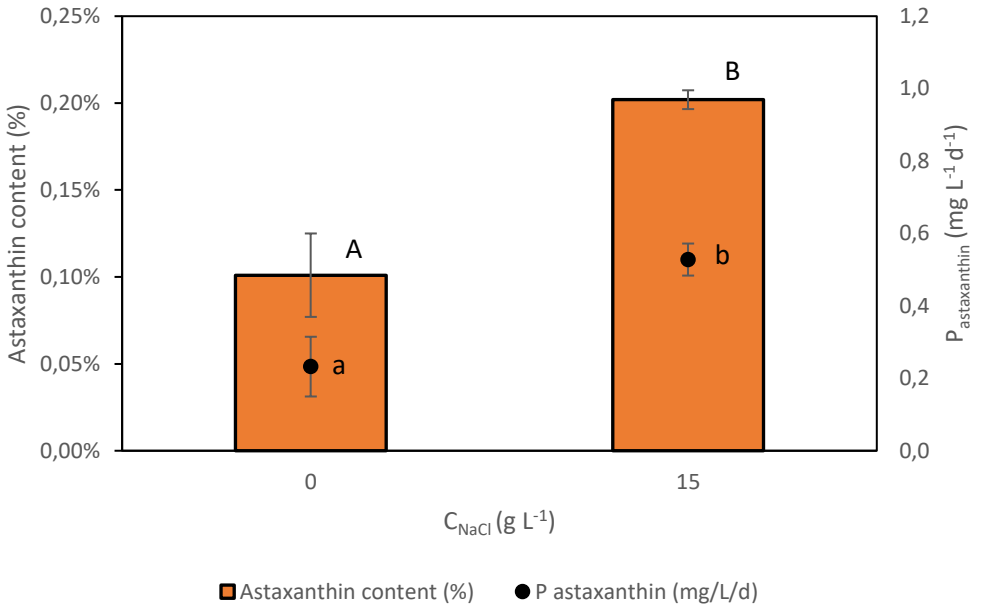

Fig. 4.3 Steady-state astaxanthin content (bars; % DW) and productivity (dots; mg L^{-1} d^{-1}) in absence or presence (15 g L^{-1}) of sodium chloride. Values are mean ± SD (n = 3). Means that do not share a letter are significantly different. Statistics refers to the same data set.

As observed in the 200-L pilot scale-PBR, a salt concentration of 15 g L^{-1} results in an increase in total carotenoid and astaxanthin content, the difference being that in the case of continuous cultivation, this increase in content is accompanied by an increase in the productivity of the product of interest. This discrepancy can be explained by the fact that, compared to the pilot-scale reactor, a lower residence time was used here (10 times lower). Furthermore, in contrast to the experiments conducted on the 200-L reactor, in the continuous experiments no reduction of the biomass concentration was observed, because at lower residence times the biomass is kept at the exponential phase of growth.

Overall, these experiments have shown that sodium chloride plays a prominent role in the accumulation of carotenoids and specifically astaxanthin, leading not only to a higher content of this valuable compound, but also to an increased astaxanthin productivity, this without affecting biomass growth. Specifically, the salt concentration used, which is comparable to the one used in the pilot-scale

reactor, when used in a continuous system, proves to be a good compromise between biomass growth and accumulation of the compound of interest. Hence, subsequent experiments were designed to assess which is the combined effect of this NaCl concentration and different inlet nitrogen concentration on biomass growth and astaxanthin productivity.

4.2 Study of the effect of inlet nitrogen concentration

The effect of the inlet nitrogen concentration on biomass growth and astaxanthin productivity was investigated. In detail, lab-scale experiments were performed with different nitrogen concentrations in the medium, keeping the sodium chloride concentration, light intensity and residence time constant. Specifically, based on the previous experiment results, the sodium chloride concentration was kept at 15 g L^{-1}.

The different inlet nitrogen concentrations used, as well as the other operating conditions, are reported in the Materials and Methods chapter in the section §2.2.3.

4.2.1 Biomass growth under different nitrogen concentrations

The Figure 4.4 shows steady-state biomass concentration and productivity at the three different inlet nitrogen concentrations tested. It can be observed that as the nitrogen concentration in the medium decreases, the growth in biomass also significantly drops, and consistently the biomass productivity. Nevertheless, it should be noted that the biomass productivity at nitrogen concentrations of 123 mg L^{-1} and 61,5 mg L^{-1} appears not to be statistically significant ($p > 0,05$).

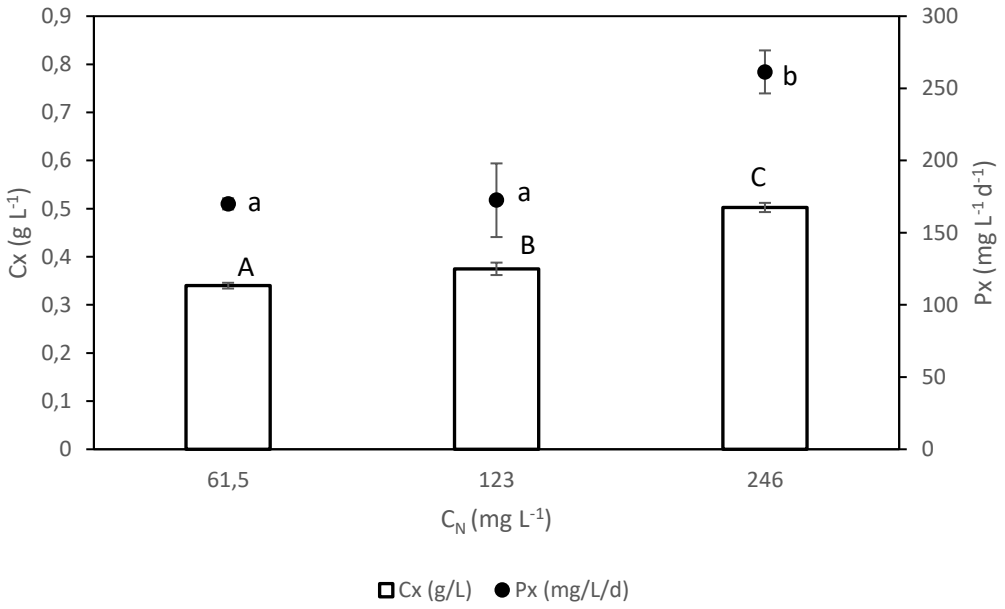

Fig. 4.4 Steady-state biomass concentration (bars; g L^{-1}) and biomass productivity (dots; mg L^{-1} d^{-1}) in absence or presence (15 g L^{-1}) of sodium chloride. Values are mean ± SD (n = 3). Means that do not share a letter are significantly different. Statistics refers to the same data set.

The decreasing trend in biomass concentration related to nitrogen limitation in the medium was similarly experienced in the pilot-scale reactor, as well as being widely documented in the literature, as discussed above.

With regard to *Chromochloris zofingiensis*, as mentioned above, to date there are no studies carried out in continuous systems, hence no comparisons can be made. It is however possible to draw a parallel with the chlorophyte *Haematococcus pluvialis*. In a study from 2005 (Del Rio *et al*.), *H. pluvialis* was cultivated under continuous conditions by varying the inlet nitrogen concentration in the medium while keeping the dilution rate and light intensity constant (0,9 d^{-1}, and 1220 mE m^{-2} s^{-1}, respectively), an approach similar to the one employed in this study. Specifically, the variation in nitrogen concentration ranged from 23,8 mg to 289,8 mg L^{-1}, with the concentration in biomass and relative productivity remaining stable up to a nitrogen concentration of 79,8 mg L^{-1}, and then decreasing significantly at lower nitrogen concentrations. In detail, the steady-state biomass concentration decreased from 1,3 to 0,7 g L^{-1} in response to the lowering of the nitrate concentration from 289,8 to 23,8 mg L^{-1}. While in the same nitrogen

concentration range, the corresponding biomass productivity decreased from 1,2 g L^{-1} d^{-1} to 0,6 g L^{-1} d^{-1}. The basic response in the presence of lower inlet nitrogen concentrations is therefore similar to the one observed with *C. zofingiensis*. These values are not comparable, however, as it must be considered that a constant salt concentration of 15 g L^{-1} is constantly present in this study.

4.2.2 Pigment and astaxanthin production under different nitrogen concentrations

The pigment profile (Fig. 4.5) shows that, similar to what was verified with biomass growth, as the nitrogen concentration in the medium drops from 246 mg L^{-1} to 123 mg L^{-1}, there is a significant decline in the total carotenoid content, as well as in chlorophyll *a* and *b* content. With the switch from 123 mg L^{-1} to 61,5 mg L^{-1}, however, there is no significant decrease, whereby the pigment content remains unchanged. In addition, the decreased biomass productivity, as well as the reduced carotenoid content, results in a decreased productivity of these (0,966 ± 0,120; 0,428 ± 0,110; 0,454 ± 0,029 mg L^{-1} d^{-1}, for 246, 123 and 61,5 mg L^{-1} of nitrogen, respectively).

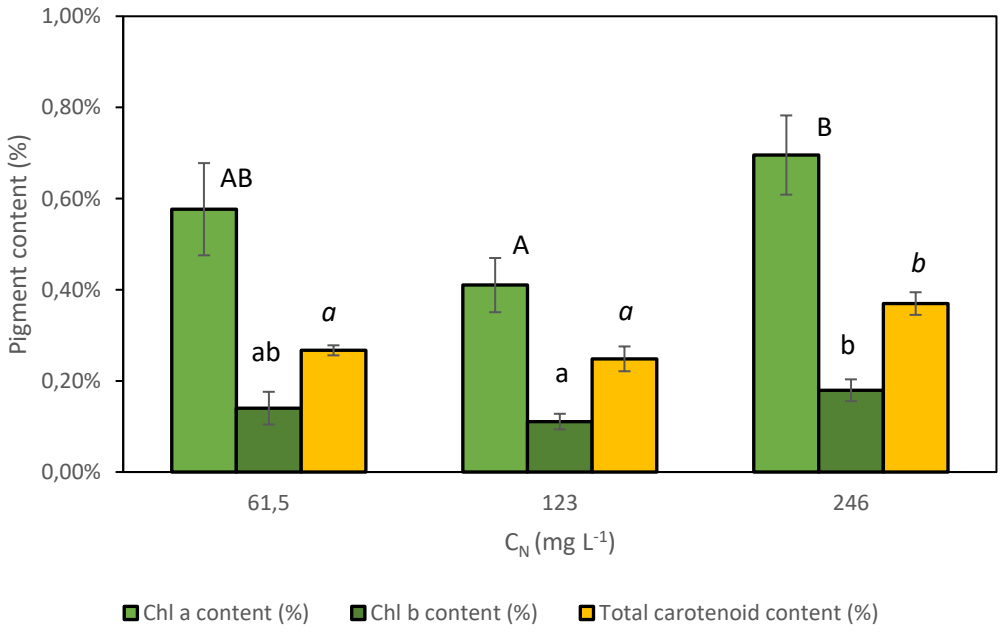

Fig. 4.5 Steady-state Chlorophyll *a*, Chlorophyll *b* and carotenoid content (% DW) in absence or presence (15 g L^{-1}) of sodium chloride. Values are mean ± SD (n = 3). Means that do not share a letter are significantly different. Statistics refers to the same data set.

Looking specifically at astaxanthin, in Figure 4.6 it is possible to observe the ketocarotenoid content and productivity. The reduction in the total carotenoid content as the nitrogen concentration decreases, resulted also in a diminished astaxanthin content, and respective productivity. Specifically, similarly to the total carotenoid trend, when the nitrogen concentration in the medium dropped from 246 mg L^{-1} to 123 mg L^{-1}, the astaxanthin content decreased in a significative manner. On the other side, with the switch from 123 mg L^{-1} to 61,5 mg L^{-1}, no significative variation occurred.

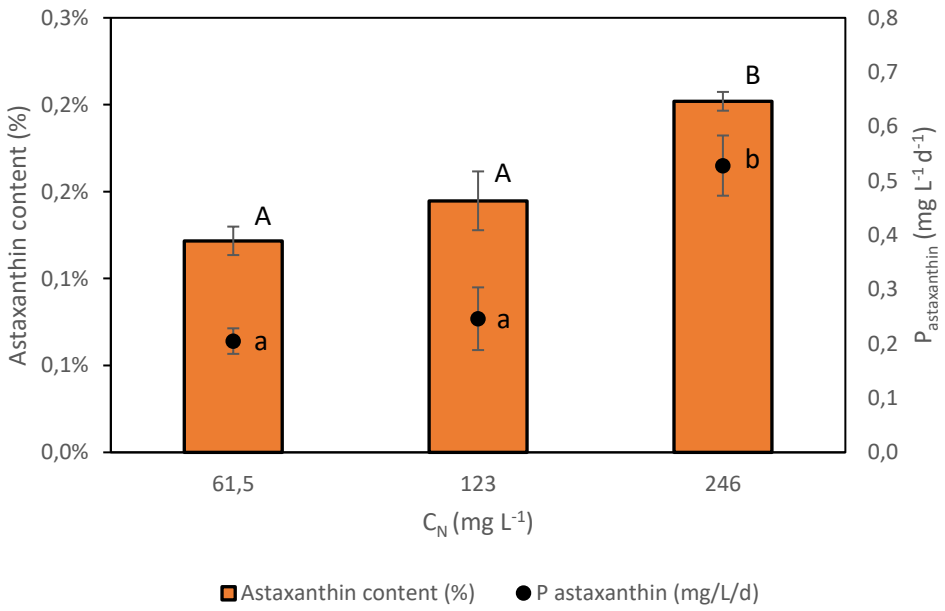

Fig. 4.6 Steady-state astaxanthin content (bars; % DW) and productivity (dots; mg L^{-1} d^{-1}) in absence or presence (15 g L^{-1}) of sodium chloride. Values are mean ± SD (n = 3). Means that do not share a letter are significantly different. Statistics refers to the same data set.

This result is in striking contrast to what was observed in the pilot-scale reactor, as well as to what has been reported in the literature for batch experiments under

similar conditions (Minyuk *et al*. 2017). This result is also in contradiction with the study by Del Rio *et al*. (2005) regarding *H. pluvialis* cited above, where a decrease in biomass concentration was observed as the inlet nitrogen concentration decreased (below 79,8 mg L^{-1}), yet accompanied by an accumulation of astaxanthin. Specifically, the highest cellular astaxanthin content (0,8% of dry biomass) was recorded for an inlet nitrogen concentration in the culture medium of 23,8 mg L^{-1}. While the maximum astaxanthin productivity (5,6 mg L^{-1} d^{-1}) was reached with a nitrogen concentration of 37,8 mg L^{-1}.

Altogether, experiments performed by varying the concentration of nitrogen in the medium have shown that in continuous systems this variable is not relevant to the production and accumulation of carotenoids and with them astaxanthin. Future experiments in continuous mode should therefore be conducted to investigate the effect of another fundamental variable, such as the availability of light and/or the residence time.

In view of this discrepancy between the results reported in the pilot-scale reactor and those obtained in continuous mode, it would be appropriate to have a modelling and quantitative approach capable of accurately describing the individual effect of the variables involved as well as their possible interactions on the response, in terms of biomass growth and carotenoid production. In this view, a Design of Experiment (DoE) statistical approach would therefore be the best method to adopt.

Chapter 5: CellDEG© cultivation

The last part of this thesis work focuses on the study of *Chromochloris zofingiensis* in the CellDEG© high-density cultivation system. The Design of Experiment (DoE) statistical approach was applied here to determine in a defined and targeted manner the effect of the combination of stressors already considered on growth and carotenoid production in the chlorophyte, with the aim of identifying the optimal combination of variables that results in the maximisation of carotenoid production. Specifically, the stress-inducing conditions included the already mentioned nitrogen limitation and salinity stress, in addition to high light.

It should be pointed out that, to date, there are no other studies of *C. zofingiensis* cultivation in the CellDEG© system in the literature, making this work the first study of the microalga in this high-density cultivation system. As this experiment is still in progress, however, only DoE results regarding biomass and some preliminary results at the pigment level will be shown and discussed hereafter.

5.1 Biomass growth in the CellDEG© system

First, the effect of the stressors has been evaluated on biomass growth. After 6-days batch cultivation, the final biomass concentration was determined and analysed with the Design-Expert software. This returned a mathematical model that enables to understand whether there are significant effects of the variables involved and their possible relationships on the outcomes, such as biomass concentration. Specifically, with regard to the latter, the Design of Experiment predicted model was first reduced, as it should be the simplest able to describe properly the dataset. The result before reduction is shown in Figure 5.1, together with the statistic parameters. A quadratic model was suggested to be the most suitable as it has a p-value lower than 0,05, a lack of fit p-value higher than 0,1 and the highest adjusted R^2. For the latter, even if the cubic model showed a higher value, it could not be considered as it resulted aliased, meaning that there were not enough runs to estimate all the coefficients.

The model reduction is based on the analysis of variance or ANOVA test, so that factors which are not statistically significant can be removed. This occurs when they show a p-value lower than 0,05 and their exclusion from the model does not reduce the predictive capability of the model. As reported in Figure 5.2, the coefficients listed, namely B, C and C^2, showed a p-value lower than 0,05. This means that the effect of these input factors on the output was statistically significant. Although the p-value of coefficient A was higher than 0,05, it was maintained in the model since its exclusion would lead to a reduction of the model predictive power. The absence of factors such as AB, BC and AC highlighted that no interaction occurs among the input factors.

Fit statistics for biomass response after reduction are shown in Figure 5.3. It can be observed that the adjusted R^2 was improved to 0,8451 and the predicted R^2 increased from 0,0785 (before reduction) to 0,7379. Adjusted R^2 is an index of the amount of variation in the dataset that is explained by the model. In this case the model describes 84,51% of the dataset variation. On the other side, predicted R^2 reflects the amount of variation in prediction that is explained by the model. It

should be within 0,2 of the adjusted R^2 to avoid model over-fitting. This condition was verified after reduction.

Source	Sequential p-value	Lack of Fit p-value	Adjusted R^2	Predicted R^2	
Linear	0,2599	0,0388	0,0940	-0,3830	
2FI	0,9428	0,0239	-0,1595	-2,0063	
Quadratic	**0,0029**	**0,2364**	**0,8069**	**0,0785**	**Suggested**
Cubic	0,2364		0,8895		**Aliased**

Fig. 5.1 Fit summary for biomass response before reduction performed with Design-Expert software.

Source	Sum of Squares	df	Mean Square	F-value	p-value	
Model	130,58	4	32,64	21,46	< 0.0001	significant
A-NaCl	6,45	1	6,45	4,24	0,0640	
B-NaNO3	8,86	1	8,86	5,82	0,0344	
C-Light intensity	25,24	1	25,24	16,59	0,0018	
C^2	90,03	1	90,03	59,19	< 0.0001	
Residual	16,73	11	1,52			
Lack of Fit	13,47	8	1,68	1,55	0,3922	not significant
Pure Error	3,26	3	1,09			
Cor Total	147,31	15				

Figure 5.2 ANOVA results for reduced quadratic model for biomass response performed with Design-Expert software.

	Std. Dev.	1,23		**R^2**	0,8864
	Mean	5,40		**Adjusted R^2**	0,8451
	C.V. %	22,83		**Predicted R^2**	0,7379
				Adeq Precision	13,8122

Figure 5.3 Fit statistics for biomass response after reduction performed with Design-Expert software.

The obtained mathematical model can be written in terms of coded or actual factors. In the first case, the factors are normalised and their values can range only between -1 and 1 according to the highest and the lowest level set for each factor during the Design of Experiment. The coded equation is useful for identifying the relative impact of the factors by comparing the factor coefficients. The higher the factor, the greater the effect of the factor on the response. Therefore, in Equation 5.1 is highlighted that light intensity (I) (C) has a stronger effect than nitrate (B) on final biomass concentration, followed by sodium chloride (A). On the other hand, the second equation (Eq 5.2), which is expressed in terms of actual factors, considers the original units for each factor and for this reason is more adequate for predictions.

$$Biomass = 3{,}03 - 0{,}90\,A + 1{,}05\,B + 1{,}78\,C + 4{,}74\,C^2 \quad \text{(Eq 5.1)}$$

$$Biomass = \ 24{,}92 - 0{,}07\,NaCl + 1{,}05\,NaNO_3 - 0{,}07\,I + 5\ 10^{-5}\,I^2 \quad \text{(Eq 5.2)}$$

In Figure 5.4 the experimental and the prediction values are reported. As they are distributed along the 45-degree line, it can be concluded that the model provides a good approximation of the dataset.

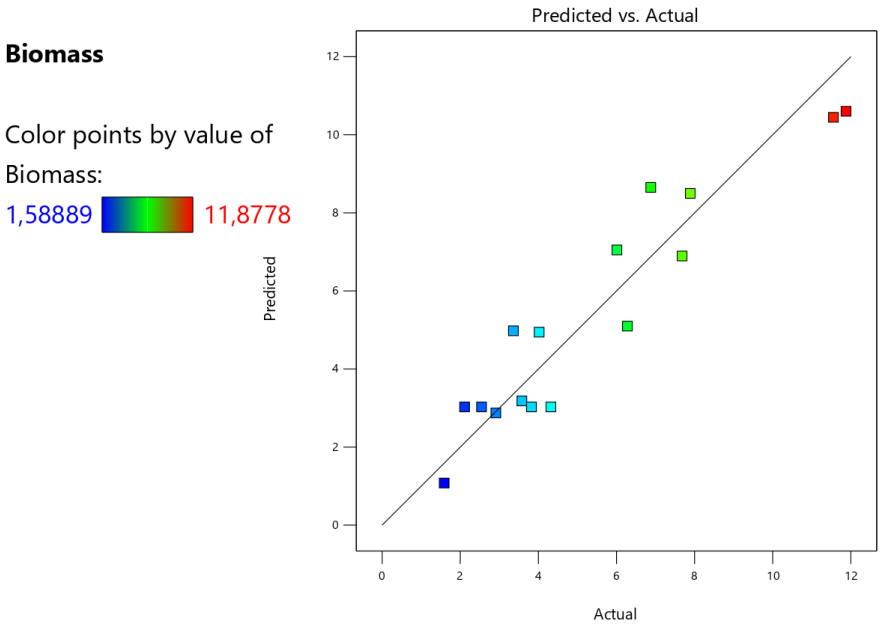

Figure 5.4 Parity plot for biomass predictive model performed with Design-Expert software.

The DoE result can be exemplified by the surface response graphs in the Figure 5.5, showing the effect of sodium chloride and nitrate concentration on biomass concentration at each light intensity level (400, 700 and 1000 µmol m^{-2} s^{-1}). These graphs allow an intuitive visualisation of the 3D relationship between independent variables and their effect on the dependent response variable.

In Figure 5.5, it can be appreciated that the reduction in biomass, reflecting the stress condition, is greater when the nitrate is reduced than when an increased amount of sodium chloride is provided. This is particularly evident from the projections of the surface on the 2D graphs showing a higher slope in the case of nitrate. Therefore, as stated before, nitrate concentration has a stronger impact than sodium chloride on biomass concentration. Additionally, the combination of nitrogen depletion in the medium ($NaNO_3$ 0 g L^{-1}) and the presence of high salt concentration (NaCl 30 g L^{-1}) led to the lowest biomass concentration among the tested conditions. On the other hand, the higher one was obtained in the opposite condition, namely with the lower level of salt (NaCl 15 g L^{-1}) and a nitrate concentration of 2 g L^{-1}.

Lastly, the isometric curves at the base of each graph provide evidence that the same biomass concentration can be obtained at lower NaCl concentrations with a simultaneous decrease in the $NaNO_3$ concentration. For instance, at 400 µmol m^{-2} s^{-1}, if the NaCl concentration is reduced from 30 to 22 g L^{-1}, to obtain the same biomass concentration the $NaNO_3$ concentration should be lowered from 0,5 to 0 g L^{-1}.

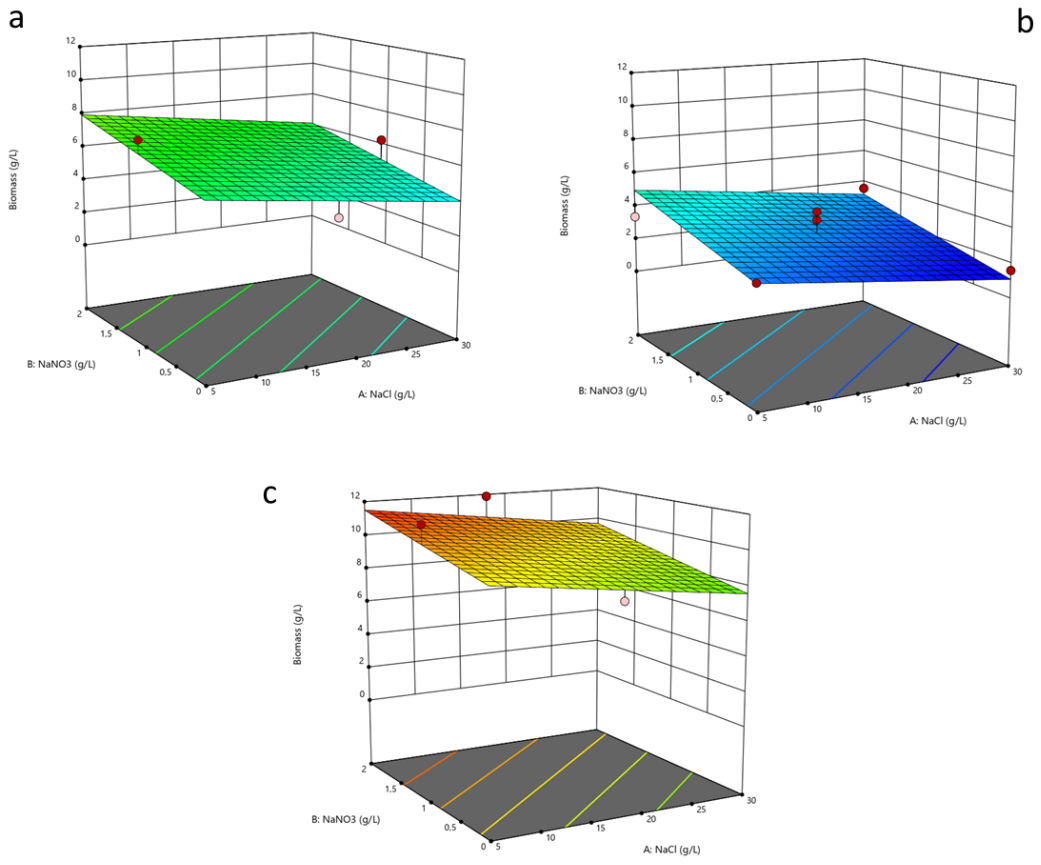

Fig. 5.5 Surface graphs showing the effect of sodium chloride and nitrate concentration (g L^{-1}) on biomass concentration (g L^{-1}). This graph was obtained by setting the light intensity at 400 µmol m^{-2} s^{-1} (a), 700 µmol m^{-2} s^{-1} (b) and 1000 µmol m^{-2} s^{-1} (c). Dots represent experimental results: red ones are above the surface, while pink ones are below.

By comparing the graphs at different light intensities, it appears that biomass growth was promoted considerably by high light (1000 µmol m^{-2} s^{-1}) during the entire culture period (6 days), while it was photo-limited at 400 µmol m^{-2} s^{-1}.

Conversely to previous outcomes reported by Lory Ascoli (Master Thesis, 2023), in which 120 µmol m^{-2} s^{-1} was suggested as the optimal light intensity, in the high-density cultivation system it seemed that light limitation occurs at higher irradiances. This could be explained by the effective design of the CellDEG© system. In fact, light and CO_2 supply as well as the mixing have been optimized to guarantee higher performances, as reported in literature (Lippi *et al*. 2018; Dienst *et al*. 2020). This can be also noticed from the biomass concentrations achieved in all the experiments performed. Indeed, they ranged between 1,589 ± 0,236 and 11,878 ± 0,236, with values higher than those disclosed in the literature. Liu *et al*. (2016) for example, in a 6-day batch study reported a maximum biomass concentration of 7,5 g L^{-1} under high light conditions, while Kou *et al*. (2020) under the same conditions reported a value of 7, 2 g L^{-1}. The values reported in this thesis are in any case mostly higher than those found under nitrogen depletion conditions by Mulders *et al*. (2014), with values of 2,5 g L^{-1}, 3,4 g L^{-1} and 4,1 g L^{-1}, at concentrations of 129, 228 and 299 mg L^{-1} of nitrogen, respectively.

Nevertheless, counterintuitively, when 700 µmol m^{-2} s^{-1} of photons were provided, the biomass result was impaired compared to the other two light intensity conditions. This may be due to the lack of standardisation of the preinoculum culture. Batch cultivation systems are sensitive to the initial physiological state of the biomass and the lack of uniformity could have a negative effect on the result. Therefore, this aspect should be taken into account in future experiments.

It should be also considered, however, that the light intensity may not have been uniform, and therefore the lesser or greater availability of light depending on the position of the cultivator on the platform may have contributed unsystematically to these results.

Several studies report the effect of different stressors on *Chromocloris zofingiensis* both alone and in combination (Liu *et al*. 2016; Kou *et al*. 2020). What is generally pointed out is the positive effect on biomass of high light intensity (350-400 µmol m^{-2} s^{-1}) compared to control conditions (70-80 µmol m^{-2} s^{-1}). Kou *et al*. (2020)

assessed the effect of salt stress (NaCl 15 g L^{-1}) highlighting that the presence of the salt induced TAG and carotenoid accumulation despite the reduction in biomass growth. However, the combination of high light (400 µmol m^{-2} s^{-1}) and salt stress produced a synergic effect with a growth consistent with the control experiment but a higher accumulation of products of interest within the biomass. A similar result was obtained by Liu *et al*. (2016) for light intensity and nitrogen-depletion, where it was suggested the use of a small amount of nitrogen (10 mg L^{-1}) and high irradiance (350 µmol m^{-2} s^{-1}) led to increased TAG and carotenoid content within biomass without compromising the growth.

Without considering results at 700 µmol m^{-2} s^{-1}, which are probably not reliable, the behaviour of biomass between 400 and 1000 µmol m^{-2} s^{-1} is consistent with what was mentioned in the previous studies. In Table 5.1 some interesting conditions are listed considering different stressors and biomass concentrations predicted with the actual equation resulting from the DoE analysis. A sodium chloride concentration of 15 g L^{-1} as a salt stress condition was considered in line with the literature. It can be observed than high light induces an increase in cellular concentration (11,78 g L^{-1}) compared to control (7,99 g L^{-1}), while salt stress and nitrogen depletion alone have a negative effect (7,27 and 5,89 g L^{-1}, respectively), which is more incisive in the latter case. The factors were also considered in combination. It is actually seen that the supply of high light together with N-depletion compensates for the impaired growth, achieving 9,68 g L^{-1} of biomass, although the result is still lower than the independent effect of light (11,78 g L^{-1}). So, as in Liu *et al*. (2016), there is a synergistic effect of the two factors. The same can be said for the combination of high light with salt stress (11,07 g L^{-1}), in agreement with what was highlighted by Kou *et al*. (2020).
In the end, the biomass outcome was also predicted in the simultaneous presence of the three stressors. It can be seen that, in this case, the biomass concentration (8.96 g L^{-1}) is greater than the control but lower than the conditions in which high light is combined only with N-depletion or salt stress.

Summing up what has been observed, therefore, light should always be considered in combination with another stressor to reduce the impairment of biomass growth induced by the latter. However, the effect of the factors should be further investigated also on pigment accumulation.

Table 5.1 Biomass concentration predicted with actual equation in different experimental conditions.

Culture condition	Light intensity ($\mu mol\ m^{-2}\ s^{-1}$)	NaCl ($g\ L^{-1}$)	$NaNO_3$ ($g\ L^{-1}$)	Predicted biomass concentration ($g\ L^{-1}$)
Control	400	5	2	7,99
N-depletion	400	5	0	5,89
Salinity stress	400	15	2	7,27
High light	1000	5	2	11,78
N-depletion + High light	1000	5	0	9,68
N-depletion + Salinity stress	400	15	0	5,17
Salinity stress + High light	1000	15	2	11,07
N-depletion + Salinity stress + High light	1000	15	0	8,96

5.2 Astaxanthin production: CellDEG© cultivation vs. continuous cultivation

The astaxanthin content and productivity have been compared between the CellDEG© and continuous experiments. 200-L PBR productivity has not been considered in this comparison as it was significantly lower. On the contrary, continuous systems are known to guarantee higher performances compared to batch systems as well as CellDEG©, which allows to reach high-density cultures. Therefore, their productivity have been compared.

Regarding the experiments conducted in the CellDEG© system, similarly to what was established for the biomass growth at the same light intensity (400 µmol m^{-2} s^{-1}), it is evident from Figure 5.6 that the main variable affecting the astaxanthin content is the nitrate concentration in the medium. In particular, it can be observed that as the nitrate concentration decreases (0 g L^{-1} $NaNO_3$, 15 g L^{-1} NaCl), there is a significative reduction ($p < 0,05$) in the astaxanthin content. On the other hand, in the experiment in which the maximum nitrate concentration in the medium is provided (2 g L^{-1} $NaNO_3$, 15 g L^{-1} NaCl), a significant increase in the astaxanthin content is observed. It also appears that the different salt concentration at the same nitrate concentration does not lead to a significant contribution to the astaxanthin content. Again, from the CellDEG© experiment with 0 g L^{-1} $NaNO_3$ and 15 g L^{-1} NaCl, it is possible to see that the combination of N-depletion and salinity stress does not result in a positive effect on astaxanthin accumulation, as well on biomass concentration (see previous paragraph). This is also confirmed by the experiments conducted in continuous mode, where it was found that a decreased nitrogen concentration, in the presence of salt, led to a reduction of both the biomass concentration and the astaxanthin content.

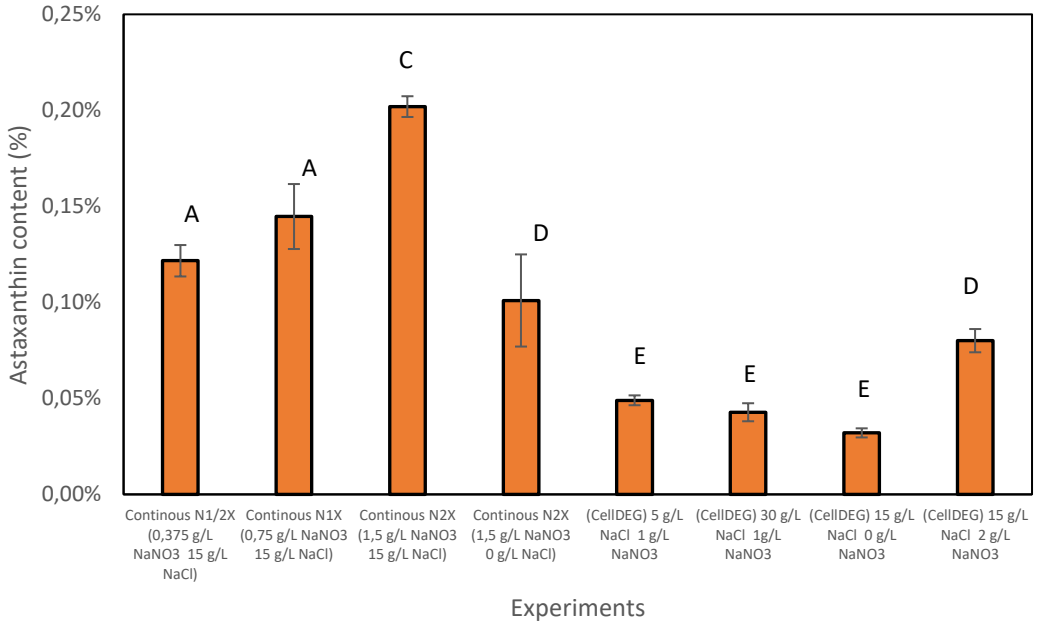

Fig. 5.6 Astaxanthin content (% DW) of the experiments performed in continuous and in the CellDEG© system. Values are mean ± SD (n = 3). Means that do not share a letter are significantly different. Statistics refers to the same data set.

On the other hand, the highest astaxanthin content, corresponding to 0,20 ± 0,01 % of DW, is found in the continuous system condition with a nitrate concentration in the medium of 1,5 g L^{-1} and a sodium chloride 15 g L^{-1}. This condition did not have the same result as the condition conducted in the CellDEG© system in similar nitrate and sodium chloride concentrations, in which the astaxanthin content was lower (0,08 ± 0,01% of DW).

It should be also noted, however, that the experiments were conducted adopting different cultivation strategies and that the light intensity employed in the continuous experiments was set at 120 µmol m^{-2} s^{-1}, while the one adopted in the CellDEG© experiments was placed at 400 µmol m^{-2} s^{-1}.

Figure 5.7 shows the astaxanthin productivity in the different experiments performed. It can be observed that the condition highlighted above as having the highest astaxanthin content is also the one with the highest astaxanthin productivity (0,528 ± 0,04 mg L^{-1} d^{-1}). Interestingly, the experiments conducted with CellDEG© appear to have a lower astaxanthin content overall than the

continuous ones, but at the same time in some cases the astaxanthin productivity is almost equal to the continuous one.

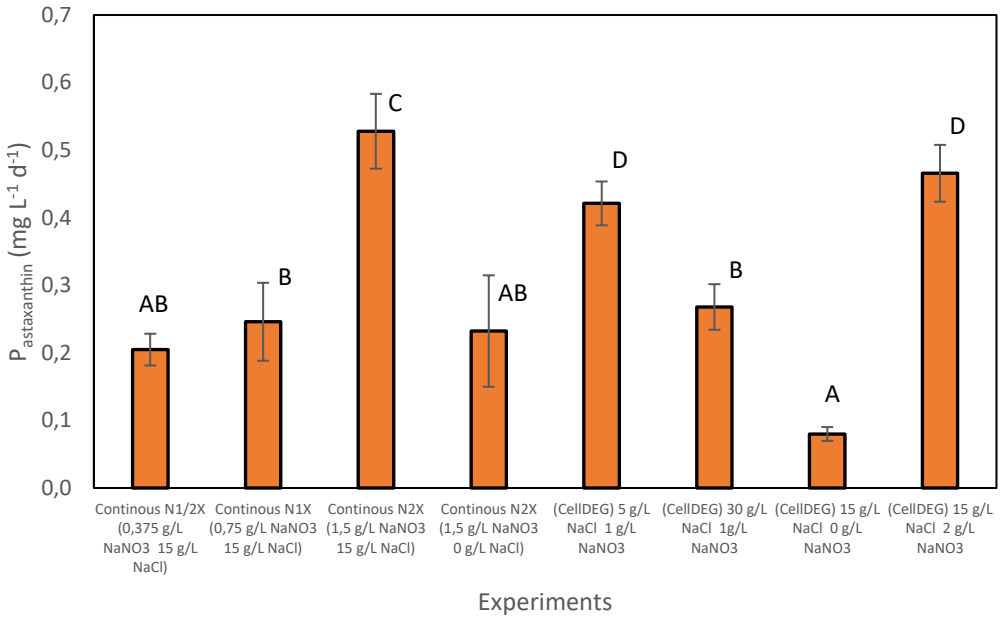

Fig. 5.7 Astaxanthin productivity (mg L^{-1} d^{-1}) of the experiments performed in continuous and in the CellDEG© system. Values are mean ± SD (n = 3). Means that do not share a letter are significantly different. Statistics refers to the same data set.

Regarding the CellDEG© experiments, it should be pointed out that, although the experiment with 5 g L^{-1} NaCl and 1 g L^{-1} $NaNO_3$, presents a significantly lower astaxanthin content than condition with 15 g L^{-1} NaCl and 2 g L^{-1} $NaNO_3$, the astaxanthin productivities of these two experiments are comparable (0,42 ± 0.03 mg L^{-1} d^{-1} and 0,47 ± 0.04 mg L^{-1} d^{-1}, respectively). This is due to a higher impairment of biomass growth in the latter case compared to the other one (5 g L^{-1} NaCl and 1 g L^{-1} $NaNO_3$).

In summary, therefore, this result seem to suggest that working in continuous may be a better strategy to achieve higher astaxanthin productivity with *C. zofingiensis*. However, further investigations to support this hypothesis are necessary.

Although so far no studies of *C. zofingiensis* in continuous systems are reported, it is possible to compare the astaxanthin productivities obtained here with values

achieved under photoautotrophic batch conditions in literature. Values not far from the maximum reported in this study (equal to 0,528 ± 0,04 mg L^{-1} d^{-1}) are reported in the work of Orosa *et al*. (2001) and Mao *et al*. (2018). Specifically, the value reached by Orosa and coworkers, equal to 0,8 mg L^{-1} d^{-1}, was obtained under combined conditions of N-starvation, high light (350 µmol m^{-2} s^{-1}) and high sodium chloride concentrations (300 mM), while the one reported by Mao *et al*. (2018), equal to 0,6 mg L^{-1} d^{-1}, was achieved under conditions of N-starvation alone. Under N-depletion conditions, on the other hand, the values appear to increase, as reported by Mulders *et al*. (2014) (1,4 mg L^{-1} d^{-1}). Higher values are obtained under conditions where N-depletion is combined with high light, reaching 2 mg L^{-1} d^{-1} (Liu *et al*. 2016). Values are similarly high under salinity stress (0,2 M) with an astaxanthin productivity of 1,7 mg L^{-1} d^{-1} (Mao *et al*. 2020). Nevertheless, the highest value reported in the literature under photoautotrophic batch conditions is the one obtained by Kou and coworkers (2020) under combined conditions of high light (400 µmol m^{-2} s^{-1}) and salt stress (0,25 M), reaching an astaxanthin productivity of 7 mg L^{-1} d^{-1}. It would therefore appear that the combination of these two stresses does not excessively affect biomass concentration, while simultaneously maximising astaxanthin content, resulting in increased astaxanthin productivity.

At this point, a comparison should be made with the chlorophyte *Haematococcus pluvialis*, the election organism for natural astaxanthin production. This microalga, similarly to *C. zofingiensis*, is able to accumulate this valuable pigment under stress-inducing conditions such as high light, nutrient limitation (specifically nitrogen limitation), and high salinity. Again, analogous to *C. zofingiensis*, the culture conditions that result in the accumulation of biomass in *H. pluvialis* differ from those that result in the accumulation of astaxanthin (Shah *et al*. 2016). Therefore, for the cultivation of this microalga and the subsequent production of astaxanthin, a two-stage strategy, consisting of a green stage followed by a red stage, is often implemented (Aflalo *et al*. 2007). In contrast to *C. zofingiensis*, however, there are some studies in the literature on the alternative one-step

approach applied to *H. pluvialis*, which, similarly to what is described in this thesis, involves the cultivation of the microalga under stress-inducing conditions in continuous mode (Del Rio *et al*. 2005). With regard to both the indoor and outdoor cultivation for astaxanthin production, the two strategies do not appear to be very different. In the work carried out by Aflalo and coworkers (2007), where a two-stage approach was applied to both indoor and outdoor cultivation, astaxanthin productivity ranged from 0,4 to 17 mg L^{-1} d^{-1}. On the other hand, for the one-step approach implemented in indoor cultivations, an average astaxanthin productivity of 20,8 mg L^{-1} d^{-1} was reported (Del Rio *et al*. 2008). While the one-step approach applied to an outdoor condition resulted in an astaxanthin yield of 8 mg L^{-1} d^{-1} (Garcia-Malea *et al*. 2009). One-step cultivation would appear to be more attractive, as it is less complicated than the two-step process, as well as allowing constant and continuous production of astaxanthin.

In general, these productivity values are, however, much higher than those obtained in the present thesis work. Yet, it should be pointed out that *H. pluvialis* exhibits a number of disadvantages that make its cultivation and astaxanthin extraction challenging (Liu *et al*. 2014). In addition to the complex life cycle, the strong dependence of *H. pluvialis* on high light intensity generally poses the problem of the inefficiency of cultivating this microalga under heterotrophic conditions, which limit its cell growth and make it more susceptible to contamination (Shah *et al*. 2016; Liu *et al*. 2014). *C. zofingiensis*, on the contrary, compared to *H. pluvialis*, exhibits a higher cell density and biomass productivity in heterotrophy, resulting in a higher astaxanthin productivity (Liu *et al*. 2014). Under heterotrophic conditions, in the presence of a glucose concentration of 40 g L^{-1}, Sun *et al*. (2019) reported, for instance, an astaxanthin content and an astaxanthin productivity of 0,92 mg g^{-1} DW and 1,10 mg L^{-1} d^{-1}, respectively. Indeed, among the advantageous features for which *C. zofingiensis* is increasingly being considered as an alternative to *H. pluvialis* for astaxanthin production is its ability to be grown under different trophic conditions (Zhang *et al*. 2021).

Chapter 6: Conclusion

The aim of this thesis was to investigate the effect of different culture conditions that lead to increased production of high-value compounds in the microalga *Chromochloris zofingiensis*, with a special focus on astaxanthin production. This strong antioxidant ketocarotenoid is produced naturally mainly from the microalga *Haematococcus pluvialis*. Due to its advantageous characteristics, *C. zofingiensis* would therefore compete as an alternative producer of this pigment. The simultaneous production of triglycerides (TAGs) under the same conditions promoting astaxanthin accumulation, makes *C. zofingiensis* also an excellent candidate for a biorefinery application, with the purpose of increasing the value of the biomass produced, while lowering production costs.

In collaboration with the company PUEVIT (PUEVIT GmbH, Dresden), this microalga was initially studied on a 200-L pilot-scale reactor, following a two-stage cultivation approach under photoautotrophic conditions. Here, the effect of nitrogen limitation and salinity stress on carotenogenesis and lipogenesis was investigated. Overall, the results showed that the stress-inducing conditions caused a significant reduction in biomass growth on the one hand, but led to an increase in carotenoid and lipid content on the other hand, without, however, leading to improved productivity. The results remain promising, however, considering the fact that to date this is the first experiment conducted on such a large scale on *C. zofingiensis*. Future improvements to enhance the system should primarily aim at optimising the so-called “green phase”, e.g. by improving the C:N ratio, also by evaluating alternative nitrogen sources, thus avoiding an excessive decrease in biomass and therefore reduced productivity of the compound of interest. A further solution would be to concentrate and accumulate the biomass before applying the stress condition. In any case, it would be important to work on the duration of the different steps, making the process as economical as

possible, and also lowering the risk of contamination. Furthermore, it would be interesting to evaluate other trophic modes, as performed in the recent study by Wood *et al*. (2023), in which a two-stage cultivation phase, consisting of an initial autotrophy phase followed by a mixotrophy phase, was successfully applied on a 65-L PBR.

Subsequent experiments were conducted on a smaller and more controlled scale, employing flat-plate PBRs operated in continuous mode. The effect of the two types of stressors mentioned above has been evaluated using the "one-factor-at-a-time" approach. The results obtained here showed how the addition of sodium chloride, unlike nitrogen limitation, resulted in an increase in carotenoid content and relative productivity, without significantly affecting biomass growth. It should be noted that the continuous cultivation strategy applied to *C. zofingiensis* is a new and still largely unexplored area of research. The present study would therefore shed new light on the possibility of cultivating this alga by employing such a cultivation strategy. Future experiments should be conducted to assess more precisely the optimal salt concentration for maximising carotenoid production. In addition, further experiments should be conducted by varying the light intensity and/or the residence time. Here again, it would be interesting to evaluate other trophic modes, such as mixotrophy.

With the ultimate aim of determining whether there is an effective interaction between the stresses employed, and, in general, to understand which are the optimal cultivation conditions for maximising carotenogenesis and lipogenesis, a Design of Experiment (DoE) statistical approach was applied to the CellDEG© high-density cultivation system. The CellDEG© cultivation system is a rather recent technology, whereas the Design of Experiment is a statistical approach that is increasingly being used on an industrial level, as it simplifies the experiment planning, reducing the number of experimental trials and consequently lowering design costs. Here, DoE results regarding biomass showed that light intensity, followed by nitrogen limitation and salt stress, was the main variable influencing

biomass growth. Additionally, although preliminary, astaxanthin outcomes suggested that the combination of salt stress with N-depletion negatively impacted the productivity of both biomass and carotenoids. The cultivation of *C. zofingiensis* in this high-density cultivation system is a novelty compared with the literature, and subsequent results will certainly give more insight into the mechanisms involved in carotenogenesis and lipogenesis of this alga under stress-inducing conditions.

Finally, astaxanthin productivity has been compared among tested systems, highlighting that continuous systems would have the highest performance.

Appendix

A1.1 Pigment profile in the CellDEG© system: preliminary results

Some preliminary results concerning the pigment profile obtained in the CellDEG© system will be described and briefly discussed below.

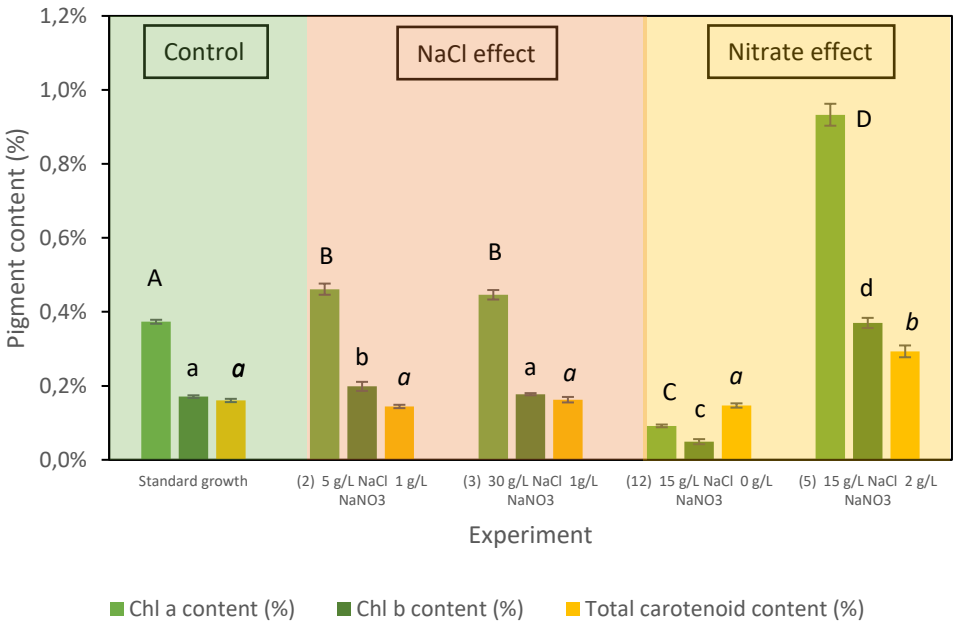

Fig. A1.1 Chlorophyll *a*, Chlorophyll *b* and carotenoid content (% DW) under different combinations of nitrate and sodium chloride concentrations with the light intensity set at 400 µmol m^{-2} s^{-1}. Values are mean ± SD (n = 3). Means that do not share a letter are significantly different. Statistics refers to the same data set.

Similarly to what was previously stated for the biomass growth at the light intensity of 400 µmol m^{-2} s^{-1} (see chapter 5 in the section §5.1), it is evident from Figure A1.1 that the main variable influencing the pigment content is the nitrate concentration in the medium. Specifically, looking at the yellow area in Figure A1.1, it is possible to observe that, as the nitrate concentration decreases (experiment 12: 15 g L^{-1} NaCl, 0 g L^{-1} $NaNO_3$), a significative reduction ($p < 0,05$) is

observed not only in the content of chlorophyll *a* and *b*, but also in the total carotenoid content compared to control condition (green area). On the other hand, in the experiment 5 (15 g L^{-1} NaCl, 2 g L^{-1} $NaNO_3$), in which the maximum nitrate concentration in the medium is provided, there is a significant increase in both chlorophyll *a*, *b* and total carotenoid content.

Conversely, it would appear that the different salt concentration, whose result is depicted in the orange area in Figure A1.1, does not lead to a significant contribution to the total carotenoid content.

References

Aflalo, C., Meshulam, Y., Zarka, A. and Boussiba, S. (2007), On the relative efficiency of two- vs. one-stage production of astaxanthin by the green alga *Haematococcus pluvialis*. Biotechnol. Bioeng., 98: 300-305. https://doi.org/10.1002/bit.21391

Ahmad, Imran, Norhayati Abdullah, Iwamoto Koji, Ali Yuzir, and Shaza Eva Muhammad. 2021. 'Evolution of Photobioreactors: A Review Based on Microalgal Perspective'. *IOP Conference Series: Materials Science and Engineering* 1142 (1): 012004. https://doi.org/10.1088/1757-899X/1142/1/012004.

Alejandro Reza-Solis, Hector, Ofelia Adriana Hernandez-Rodriguez, Andres Francisco Martinez-Rosales, and Damaaris Leopoldina Ojeda-Barrios. 2023. 'Applications of Microalgae in Five Areas of Biotechnology'. *Phyton* 92 (10): 2737–59. https://doi.org/10.32604/phyton.2023.029851.

Andersen, Robert A., and Phycological Society of America, eds. 2009. *Algal Culturing Techniques*. Nachdr. Amsterdam Heidelberg: Elsevier Academic Press.

Ascoli, Lory. 2023. Master thesis

B. Kell, Douglas, Gerard H. Markx, Chris L. Davey, and Robert W. Todd. 1990. 'Real-Time Monitoring of Cellular Biomass: Methods and Applications'. *TrAC Trends in Analytical Chemistry* 9 (6): 190–94. https://doi.org/10.1016/0165-9936(90)87042-K.

Béchet, Quentin, Andy Shilton, and Benoit Guieysse. 2013. 'Modeling the Effects of Light and Temperature on Algae Growth: State of the Art and Critical Assessment for Productivity Prediction during Outdoor Cultivation'. *Biotechnology Advances* 31 (8): 1648–63. https://doi.org/10.1016/j.biotechadv.2013.08.014.

Benner, Philipp, Lisa Meier, Annika Pfeffer, Konstantin Krüger, José Enrique Oropeza Vargas, and Dirk Weuster-Botz. 2022. 'Lab-Scale Photobioreactor

Systems: Principles, Applications, and Scalability'. *Bioprocess and Biosystems Engineering* 45 (5): 791–813. https://doi.org/10.1007/s00449-022-02711-1.

Borella, Lisa, Eleonora Sforza, and Alberto Bertucco. 2021. 'Effect of Residence Time in Continuous Photobioreactor on Mass and Energy Balance of Microalgal Protein Production'. *New Biotechnology* 64 (September): 46–53. https://doi.org/10.1016/j.nbt.2021.05.006.

Chandrasekhar, K., Tirath Raj, S.V. Ramanaiah, Gopalakrishnan Kumar, J. Rajesh Banu, Sunita Varjani, Pooja Sharma, Ashok Pandey, Sunil Kumar, and Sang-Hyoun Kim. 2022. 'Algae Biorefinery: A Promising Approach to Promote Microalgae Industry and Waste Utilization'. *Journal of Biotechnology* 345 (February): 1–16. https://doi.org/10.1016/j.jbiotec.2021.12.008.

Chanquia, Santiago N., Guillem Vernet, and Selin Kara. 2022. 'Photobioreactors for Cultivation and Synthesis: Specifications, Challenges, and Perspectives'. *Engineering in Life Sciences* 22 (12): 712–24. https://doi.org/10.1002/elsc.202100070.

Christaki, Efterpi, Panagiota Florou-Paneri, and Eleftherios Bonos. 2011. 'Microalgae: A Novel Ingredient in Nutrition'. *International Journal of Food Sciences and Nutrition* 62 (8): 794–99. https://doi.org/10.3109/09637486.2011.582460.

Daneshvar, Ehsan, Yong Sik Ok, Samad Tavakoli, Binoy Sarkar, Sabry M. Shaheen, Hui Hong, Yongkang Luo, Jörg Rinklebe, Hocheol Song, and Amit Bhatnagar. 2021a. 'Insights into Upstream Processing of Microalgae: A Review'. *Bioresource Technology* 329 (June): 124870. https://doi.org/10.1016/j.biortech.2021.124870.

———. 2021b. 'Insights into Upstream Processing of Microalgae: A Review'. *Bioresource Technology* 329 (June): 124870. https://doi.org/10.1016/j.biortech.2021.124870.

Del Campo, J. A., H. Rodriguez, J. Moreno, M. A. Vargas, J. Rivas, and M. G. Guerrero. 2004. 'Accumulation of Astaxanthin and Lutein in Chlorella

Zofingiensis (Chlorophyta)'. *Applied Microbiology and Biotechnology* 64 (6): 848–54. https://doi.org/10.1007/s00253-003-1510-5.

Del Rio, E., Acién, F.G., García-Malea, M.C., Rivas, J., Molina-Grima, E. and Guerrero, M.G. (2005), Efficient one-step production of astaxanthin by the microalga *Haematococcus pluvialis* in continuous culture. Biotechnol. Bioeng., 91: 808-815. https://doi.org/10.1002/bit.20547

Del Río, E., Acién, F.G., García-Malea, M.C., Rivas, J., Molina-Grima, E. and Guerrero, M.G. (2008), Efficiency assessment of the one-step production of astaxanthin by the microalga *Haematococcus pluvialis*. Biotechnol. Bioeng., 100: 397-402. https://doi.org/10.1002/bit.21770

Dienst, Dennis, Julian Wichmann, Oliver Mantovani, João S. Rodrigues, and Pia Lindberg. 2020. 'High Density Cultivation for Efficient Sesquiterpenoid Biosynthesis in Synechocystis Sp. PCC 6803'. *Scientific Reports* 10 (1): 5932. https://doi.org/10.1038/s41598-020-62681-w.

Fernandes, Bruno D., Andre Mota, Jose A. Teixeira, and Antonio A. Vicente. 2015. 'Continuous Cultivation of Photosynthetic Microorganisms: Approaches, Applications and Future Trends'. *Biotechnology Advances* 33 (6): 1228–45. https://doi.org/10.1016/j.biotechadv.2015.03.004.

Franke, Sabine, Juliane Steingröwer, Thomas Walther, and Felix Krujatz. 2022. 'The Oxygen Paradigm—Quantitative Impact of High Concentrations of Dissolved Oxygen on Kinetics and Large-Scale Production of Arthrospira Platensis'. *ChemEngineering* 6 (1): 14. https://doi.org/10.3390/chemengineering6010014.

García-Malea, M.C., Acién, F.G., Del Río, E., Fernández, J.M., Cerón, M.C., Guerrero, M.G. and Molina-Grima, E. (2009), Production of astaxanthin by *Haematococcus pluvialis*: Taking the one-step system outdoors. Biotechnol. Bioeng., 102: 651-657. https://doi.org/10.1002/bit.22076

Gateau, Helene, Katalin Solymosi, Justine Marchand, and Benoit Schoefs. 2017. 'Carotenoids of Microalgae Used in Food Industry and Medicine'. *Mini-Reviews in Medicinal Chemistry* 17 (13). https://doi.org/10.2174/1389557516666160808123841.

Hewavitharana, Geeth G., Dilini N. Perera, S.B. Navaratne, and I. Wickramasinghe. 2020. 'Extraction Methods of Fat from Food Samples and Preparation of Fatty Acid Methyl Esters for Gas Chromatography: A Review'. *Arabian Journal of Chemistry* 13 (8): 6865–75. https://doi.org/10.1016/j.arabjc.2020.06.039.

Ip, Po-Fung, Ka-Ho Wong, and Feng Chen. 2004. 'Enhanced Production of Astaxanthin by the Green Microalga Chlorella Zofingiensis in Mixotrophic Culture'. *Process Biochemistry* 39 (11): 1761–66. https://doi.org/10.1016/j.procbio.2003.08.003.

Jankovic, Aleksandar, Gaurav Chaudhary, and Francesco Goia. 2021. 'Designing the Design of Experiments (DOE) – An Investigation on the Influence of Different Factorial Designs on the Characterization of Complex Systems'. *Energy and Buildings* 250 (November): 111298. https://doi.org/10.1016/j.enbuild.2021.111298.

Juneja, Ankita, Ruben Ceballos, and Ganti Murthy. 2013. 'Effects of Environmental Factors and Nutrient Availability on the Biochemical Composition of Algae for Biofuels Production: A Review'. *Energies* 6 (9): 4607–38. https://doi.org/10.3390/en6094607.

Kaur, Manpreet, Surekha Bhatia, Urmila Gupta, Eric Decker, Yamini Tak, Manoj Bali, Vijai Kumar Gupta, Rouf Ahmad Dar, and Saroj Bala. 2023. 'Microalgal Bioactive Metabolites as Promising Implements in Nutraceuticals and Pharmaceuticals: Inspiring Therapy for Health Benefits'. *Phytochemistry Reviews* 22 (4): 903–33. https://doi.org/10.1007/s11101-022-09848-7.

Khan, Muhammad Imran, Jin Hyuk Shin, and Jong Deog Kim. 2018. 'The Promising Future of Microalgae: Current Status, Challenges, and Optimization of a Sustainable and Renewable Industry for Biofuels, Feed, and Other Products'. *Microbial Cell Factories* 17 (1): 36. https://doi.org/10.1186/s12934-018-0879-x.

Khoo, Kuan Shiong, Sze Ying Lee, Chien Wei Ooi, Xiaoting Fu, Xiaoling Miao, Tau Chuan Ling, and Pau Loke Show. 2019. 'Recent Advances in Biorefinery of

Astaxanthin from Haematococcus Pluvialis'. *Bioresource Technology* 288 (September): 121606. https://doi.org/10.1016/j.biortech.2019.121606.

Kou, Yaping, Meijing Liu, Peipei Sun, Zhaoqi Dong, and Jin Liu. 2020. 'High Light Boosts Salinity Stress-Induced Biosynthesis of Astaxanthin and Lipids in the Green Alga Chromochloris Zofingiensis'. *Algal Research* 50 (September): 101976. https://doi.org/10.1016/j.algal.2020.101976.

Kratzer, Regina, and Michael Murkovic. 2021. 'Food Ingredients and Nutraceuticals from Microalgae: Main Product Classes and Biotechnological Production'. *Foods* 10 (7): 1626. https://doi.org/10.3390/foods10071626.

Kusmayadi, Adi, Yoong Kit Leong, Hong-Wei Yen, Chi-Yu Huang, and Jo-Shu Chang. 2021a. 'Microalgae as Sustainable Food and Feed Sources for Animals and Humans – Biotechnological and Environmental Aspects'. *Chemosphere* 271 (May): 129800. https://doi.org/10.1016/j.chemosphere.2021.129800.

———. 2021b. 'Microalgae as Sustainable Food and Feed Sources for Animals and Humans – Biotechnological and Environmental Aspects'. *Chemosphere* 271 (May): 129800. https://doi.org/10.1016/j.chemosphere.2021.129800.

Lari, Zahra, and Fatemeh Khosravitabar. 2020. 'A Comparative Review on Different Trophic Modes and Usable Carbon Sources for Microalgae Cultivation, Approaching to Optimize Lipid Production in Trade Scale'. *Systematic Bioscience and Engineering*, April, 16–26. https://doi.org/10.37256/sbe.112021293.

Lippi, Luca, Lars Bähr, Arne Wüstenberg, Annegret Wilde, and Ralf Steuer. 2018. 'Exploring the Potential of High-Density Cultivation of Cyanobacteria for the Production of Cyanophycin'. *Algal Research* 31 (April): 363–66. https://doi.org/10.1016/j.algal.2018.02.028.

Liu, Jin, Junchao Huang, Zheng Sun, Yujuan Zhong, Yue Jiang, and Feng Chen. 2011. 'Differential Lipid and Fatty Acid Profiles of Photoautotrophic and Heterotrophic Chlorella Zofingiensis: Assessment of Algal Oils for Biodiesel Production'. *Bioresource Technology* 102 (1): 106–10. https://doi.org/10.1016/j.biortech.2010.06.017.

Liu, Jin, Xuemei Mao, Wenguang Zhou, and Michael T. Guarnieri. 2016. 'Simultaneous Production of Triacylglycerol and High-Value Carotenoids by the Astaxanthin-Producing Oleaginous Green Microalga Chlorella Zofingiensis'. *Bioresource Technology* 214 (August): 319–27. https://doi.org/10.1016/j.biortech.2016.04.112.

Liu, Jin, Zheng Sun, Henri Gerken, Zheng Liu, Yue Jiang, and Feng Chen. 2014. 'Chlorella Zofingiensis as an Alternative Microalgal Producer of Astaxanthin: Biology and Industrial Potential'. *Marine Drugs* 12 (6): 3487–3515. https://doi.org/10.3390/md12063487.

Liu, Jin, Zheng Sun, Xuemei Mao, Henri Gerken, Xiaofei Wang, and Wenqiang Yang. 2019. 'Multiomics Analysis Reveals a Distinct Mechanism of Oleaginousness in the Emerging Model Alga *Chromochloris Zofingiensis*'. *The Plant Journal* 98 (6): 1060–77. https://doi.org/10.1111/tpj.14302.

Mao, Xuemei, Tao Wu, Dongzhe Sun, Zhao Zhang, and Feng Chen. 2018. 'Differential Responses of the Green Microalga Chlorella Zofingiensis to the Starvation of Various Nutrients for Oil and Astaxanthin Production'. *Bioresource Technology* 249 (February): 791–98. https://doi.org/10.1016/j.biortech.2017.10.090.

Mao, Xuemei, Yu Zhang, Xiaofei Wang, and Jin Liu. 2020. 'Novel Insights into Salinity-Induced Lipogenesis and Carotenogenesis in the Oleaginous Astaxanthin-Producing Alga Chromochloris Zofingiensis: A Multi-Omics Study'. *Biotechnology for Biofuels* 13 (1): 73. https://doi.org/10.1186/s13068-020-01714-y.

Minyuk, Galina, Elina Chelebieva, Irina Chubchikova, Natalia Dantsyuk, Irina Drobetskaya, Evgenii Sakhon, Konstantin Chekanov, and Alexei Solovchenko. 2017. 'Stress-Induced Secondary Carotenogenesis in Coelastrella Rubescens (Scenedesmaceae, Chlorophyta), a Producer of Value-Added Keto-Carotenoids'. *ALGAE* 32 (3): 245–59. https://doi.org/10.4490/algae.2017.32.8.6.

Minyuk, Galina, Roman Sidorov, and Alexei Solovchenko. 2020. 'Effect of Nitrogen Source on the Growth, Lipid, and Valuable Carotenoid Production in the

Green Microalga Chromochloris Zofingiensis'. *Journal of Applied Phycology* 32 (2): 923–35. https://doi.org/10.1007/s10811-020-02060-0.

Mohsenpour, Seyedeh Fatemeh, Sebastian Hennige, Nicholas Willoughby, Adebayo Adeloye, and Tony Gutierrez. 2021. 'Integrating Micro-Algae into Wastewater Treatment: A Review'. *Science of The Total Environment* 752 (January): 142168. https://doi.org/10.1016/j.scitotenv.2020.142168.

Mulders, Kim J.M., Jorijn H. Janssen, Dirk E. Martens, René H. Wijffels, and Packo P. Lamers. 2014. 'Effect of Biomass Concentration on Secondary Carotenoids and Triacylglycerol (TAG) Accumulation in Nitrogen-Depleted Chlorella Zofingiensis'. *Algal Research* 6 (October): 8–16. https://doi.org/10.1016/j.algal.2014.08.006.

Nair, Anagha, Ankesh Ahirwar, Shashikala Singh, Reeta Lodhi, Aishwarya Lodhi, Anshuman Rai, Dipak A Jadhav, et al. 2023. 'Astaxanthin as a King of Ketocarotenoids: Structure, Synthesis, Accumulation, Bioavailability and Antioxidant Properties'. *Marine Drugs* 21 (3): 176. https://doi.org/10.3390/md21030176.

Orosa, M., J.F. Valero, C. Herrero, and J. Abalde. 2001. '[No Title Found]'. *Biotechnology Letters* 23 (13): 1079–85. https://doi.org/10.1023/A:1010510508384.

Pal, Preeti, Kit Wayne Chew, Hong-Wei Yen, Jun Wei Lim, Man Kee Lam, and Pau Loke Show. 2019. 'Cultivation of Oily Microalgae for the Production of Third-Generation Biofuels'. *Sustainability* 11 (19): 5424. https://doi.org/10.3390/su11195424.

Ravindran, Balasubramani, Sanjay Gupta, Won-Mo Cho, Jung Kim, Sang Lee, Kwang-Hwa Jeong, Dong Lee, and Hee-Chul Choi. 2016. 'Microalgae Potential and Multiple Roles—Current Progress and Future Prospects—An Overview'. *Sustainability* 8 (12): 1215. https://doi.org/10.3390/su8121215.

Reichelt, Niklas, Dorian Leger, Mareike Daubert, Paolo Ruffino, Thomas Pröschold, and Tatyana Darienko. 2021. 'Epigenomic Stability Assessment during Cryopreservation and Physiology among Various Strains of Chromochloris

Zofingiensis (Chlorophyceae) and Their Genetic Variability Revealed by AFLP and MS-AFLP'. *Journal of Applied Phycology* 33 (4): 2327–40. https://doi.org/10.1007/s10811-021-02468-2.

Richmond, Amos, ed. 2007. *Handbook of Microalgal Culture: Biotechnology and Applied Phycology*. Nachdr. Oxford: Blackwell Science.

Roth, Melissa S., Shawn J. Cokus, Sean D. Gallaher, Andreas Walter, David Lopez, Erika Erickson, Benjamin Endelman, et al. 2017. 'Chromosome-Level Genome Assembly and Transcriptome of the Green Alga *Chromochloris Zofingiensis* Illuminates Astaxanthin Production'. *Proceedings of the National Academy of Sciences* 114 (21). https://doi.org/10.1073/pnas.1619928114.

Shah, Md. Mahfuzur R., Yuanmei Liang, Jay J. Cheng, and Maurycy Daroch. 2016. 'Astaxanthin-Producing Green Microalga Haematococcus Pluvialis: From Single Cell to High Value Commercial Products'. *Frontiers in Plant Science* 7 (April). https://doi.org/10.3389/fpls.2016.00531.

Sun, Zheng, Yu Zhang, Li-ping Sun, and Jin Liu. 2019. 'Light Elicits Astaxanthin Biosynthesis and Accumulation in the Fermented Ultrahigh-Density *Chlorella Zofinginesis*'. *Journal of Agricultural and Food Chemistry* 67 (19): 5579–86. https://doi.org/10.1021/acs.jafc.9b01176.

Takenaka, Hiroyuki, and Yuji Yamaguchi. 2014. 'Commercial-scale Culturing of Cyanobacteria: An Industrial Experience'. In *Cyanobacteria*, edited by Naveen K. Sharma, Ashwani K. Rai, and Lucas J. Stal, 1st ed., 293–301. Wiley. https://doi.org/10.1002/9781118402238.ch18.

Trentin, Giulia, Veronica Lucato, Eleonora Sforza, and Alberto Bertucco. 2021. 'Stabilizing Autotrophic Cyanophycin Production in Continuous Photobioreactors'. *Algal Research* 60 (December): 102518. https://doi.org/10.1016/j.algal.2021.102518.

Trentin, Giulia, Francesca Piazza, Marta Carletti, Boris Zorin, Inna Khozin-Goldberg, Alberto Bertucco, and Eleonora Sforza. 2023. 'Fixing N2 into Cyanophycin: Continuous Cultivation of Nostoc Sp. PCC 7120'. *Applied Microbiology and*

Biotechnology 107 (1): 97–110. https://doi.org/10.1007/s00253-022-12292-4.

Ugwu, C.U., H. Aoyagi, and H. Uchiyama. 2008. 'Photobioreactors for Mass Cultivation of Algae'. *Bioresource Technology* 99 (10): 4021–28. https://doi.org/10.1016/j.biortech.2007.01.046.

Vale, Miguel A., António Ferreira, José C.M. Pires, and Ana L. Gonçalves. 2020. 'CO2 Capture Using Microalgae'. In *Advances in Carbon Capture*, 381–405. Elsevier. https://doi.org/10.1016/B978-0-12-819657-1.00017-7.

Vanthoor-Koopmans, Marieke, Rene H. Wijffels, Maria J. Barbosa, and Michel H.M. Eppink. 2013. 'Biorefinery of Microalgae for Food and Fuel'. *Bioresource Technology* 135 (May): 142–49. https://doi.org/10.1016/j.biortech.2012.10.135.

Villaró, Silvia, Martina Ciardi, Ainoa Morillas-España, Ana Sánchez-Zurano, Gabriel Acién-Fernández, and Tomas Lafarga. 2021. 'Microalgae Derived Astaxanthin: Research and Consumer Trends and Industrial Use as Food'. *Foods* 10 (10): 2303. https://doi.org/10.3390/foods10102303.

Vozelj, Pia. 2023. "Cultivation of the Carotenoid-Producing Microalgae Chromochloris Zofingiensis at Laboratory and Pilot Scale." Master's thesis, Winterthur: ZHAW Zürcher Hochschule für Angewandte Wissenschaften. https://doi.org/10.21256/zhaw-28451.

Wang, Bei, Christopher Q. Lan, and Mark Horsman. 2012. 'Closed Photobioreactors for Production of Microalgal Biomasses'. *Biotechnology Advances* 30 (4): 904–12. https://doi.org/10.1016/j.biotechadv.2012.01.019.

Wellburn, Alan R. 1994. 'The Spectral Determination of Chlorophylls a and b, as Well as Total Carotenoids, Using Various Solvents with Spectrophotometers of Different Resolution'. *Journal of Plant Physiology* 144 (3): 307–13. https://doi.org/10.1016/S0176-1617(11)81192-2.

Wood, Eleanor E., Michael E. Ross, Sébastien Jubeau, Valéria Montalescot, Karen MacKechnie, Ryan E. Marchington, Matthew P. Davey, Sharon McNeill, Callum Hamilton, and Michele S. Stanley. 2023. 'From Green to Orange:

The Change in Biochemical Composition of Phototrophic-Mixotrophic Chromochloris Zofingiensis in Pilot-Scale Photobioreactors'. *Algal Research* 75 (September): 103238. https://doi.org/10.1016/j.algal.2023.103238.

Wood, Eleanor E., Michael E. Ross, Sébastien Jubeau, Valéria Montalescot, and Michele S. Stanley. 2022. 'Progress towards a Targeted Biorefinery of Chromochloris Zofingiensis: A Review'. *Biomass Conversion and Biorefinery*, June. https://doi.org/10.1007/s13399-022-02955-7.

Yin, Zhihong, Liandong Zhu, Shuangxi Li, Tianyi Hu, Ruoyu Chu, Fan Mo, Dan Hu, Chenchen Liu, and Bin Li. 2020. 'A Comprehensive Review on Cultivation and Harvesting of Microalgae for Biodiesel Production: Environmental Pollution Control and Future Directions'. *Bioresource Technology* 301 (April): 122804. https://doi.org/10.1016/j.biortech.2020.122804.

Zhang, Yu, Ying Ye, Fan Bai, and Jin Liu. 2021. 'The Oleaginous Astaxanthin-Producing Alga Chromochloris Zofingiensis: Potential from Production to an Emerging Model for Studying Lipid Metabolism and Carotenogenesis'. *Biotechnology for Biofuels* 14 (1): 119. https://doi.org/10.1186/s13068-021-01969-z.

Zuccaro, Gaetano, Abu Yousuf, Antonino Pollio, and Jean-Philippe Steyer. 2020. 'Microalgae Cultivation Systems'. In *Microalgae Cultivation for Biofuels Production*, 11–29. Elsevier. https://doi.org/10.1016/B978-0-12-817536-1.00002-3.